DOE/PC/90364-T6
(DE93014939)
Distribution Category UC-105

Flue Gas Conditioning for Improved Particle Collection in Electrostatic Precipitators

First Topical Report

Results of Laboratory Screening of Additives

Contract No. DE-AC22-91PC90364

Prepared for:

U.S. Department of Energy
Pittsburgh Energy Technology Center
Pittsburgh, PA 15236

Project Officer: Mr. Thomas Brown

Prepared by

Michael D. Durham, Ph.D.

ADA Technologies, Inc.
304 Inverness Way So.
Englewood, CO 80112

(303) 792-5615

ADA Report 4300-93-T1

April 16, 1993

Table of Contents

I. Executive Summary

ADA Technologies, Inc. (ADA) has completed several tasks of a program to evaluate additives to improve the collection of fine particles in electrostatic precipitators (ESPs). Additives will be injected (in liquid form) into the flue gas of coal-fired power plants where they will contact flyash particles and render them more cohesive. This process will improve the collectability of these particles using existing electrostatic precipitators (ESPs).

The testing and data gathering portions of the program are being conducted in phases, where each phase builds upon and is a scale up from the previous phase. The purpose of this Topical Report is to summarize the work performed during screening tests and laboratory-scale evaluations of candidate additives.

A review of literature on adhesives provided a list of potential additives to be evaluated during the program. The criteria used in selecting candidate additives included: the candidates must be non-toxic and substantially different from traditional additives (SO_3 and NH_3); the candidates must be in a form that can be injected into flue gas; the economics for using the additives must be attractive in comparison to the alternatives; and the additive injection system must be easy to retrofit into existing plants. The identified additives included families of naturally occurring products and compounds used in food and cosmetic industries.

Candidate additives were obtained from suppliers for an initial screening test. This test involved mixing dilute water solutions of the additives with flyash. The mixture was heated in an oven to evaporate the water, and the resulting solids were visually inspected. The additives which produced the most predominant agglomerated solid masses with the flyash were then subjected to laboratory-scale precipitation tests.

A laboratory-scale test apparatus (3 acfm) was assembled to provide test atmospheres for evaluating additives. Several modifications of the equipment were necessary in order to produce consistent and reproducible test conditions. The ADA Resistivity Device was used as the test chamber to precipitate flyash for the evaluation. The Resistivity Device also provided a means for quantifying the effects produced by the candidate additives in terms of precipitated dust layer thickness. Over twenty different additives were evaluated using the laboratory-scale fixture. Four were found to produce significant improvements in flyash precipitation rates compared to baseline (no additives) conditions. An economic analysis is in progress to evaluate the costs associated with these four additives. These additives will be prioritized for bench-scale testing (100 acfm) at Consolidation Coal Company based on the economic analysis.

Photographs presented in Figure I-1 show an example of flyash precipitation rates observed during a laboratory-scale test. A point-to-plane precipitator was used for these tests. Flyash precipitated under a baseline test condition (no additives) is shown on the left. The photograph on the right shows flyash precipitated under identical testing conditions with the addition of an additive. A significant improvement in the quantity of flyash collected during the additive test is visibly evident. Quantitative measurements of the thickness of the precipitated layers showed that four aditives produced significant improvements in precipitation rates.

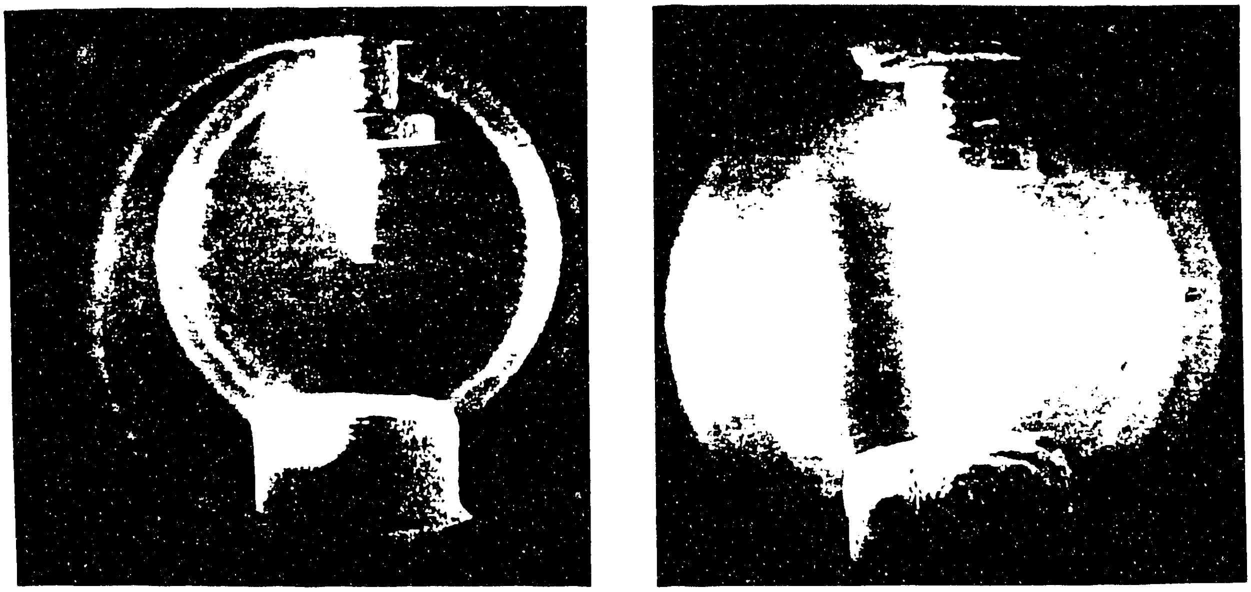

a. Baseline **b. With Additives**

Figure I-1. Effect of Additives on the Characteristics of Precipitated Dust.

The Insitec particle analyzer was also evaluated during the initial phase of the program. This is a key item of test equipment that will be used during the bench- and pilot-scale testing phases of the overall program. Test results, summarized in Figure I-2, showed that the analyzer will provide accurate sizing and counting information for particles in the size range of interest which is ≤ 10 μm in diameter.

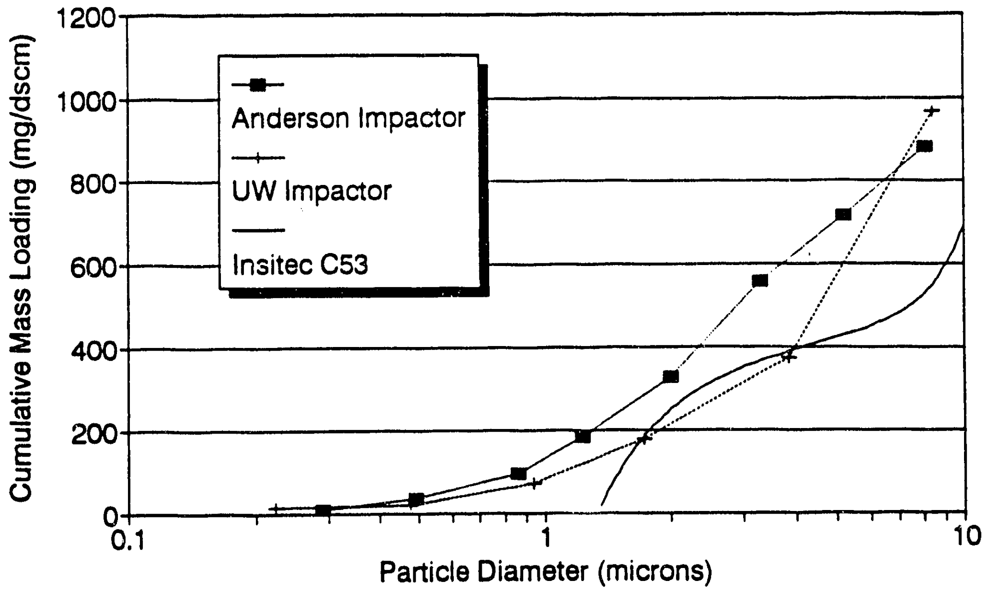

Figure I-2. Comparison of the Insitec Analyzer With Cascade Impactor Particle Sizing Samplers.

Based on the results obtained to date, it is recommended that bench-scale testing be conducted using four of the candidate additives identified thus far. One or more of the candidates may be disqualified based on an economic analysis. Key components of the bench-scale system are currently being assembled and checked in preparation for the testing at Consolidation Coal Company.

II. Introduction

Electrostatic precipitators (ESP) serve as the primary air pollution control device for the majority of coal-fired utility boilers in the Eastern and Midwestern regions of the United States. Since most of these ESPs are collecting flyash generated from medium- and high-sulfur coal, they are not experiencing operational limitations which are common when treating high-resistivity particles and are performing at an efficiency that is as high as could be expected.

However, there are indications that the collection efficiency could be improved with flue gas conditioning. Conditioning is commonly used for solving operational problems associated with high-resistivity dusts. The purpose of conditioning for low- and moderate-resistivity applications is to increase the cohesive characteristics of the dust. Flue gas conditioning that increases particle cohesion has the potential to improve overall collection efficiency because a large percentage of particulate emissions from a well-performing ESP is due to reentrainment. Improved ESP performance should result if particle reentrainment could be reduced by making the particles more cohesive. This could produce a significant reduction in emissions from an ESP from the following mechanisms:

- Reduced erosion-type reentrainment
- Reduced rapping emissions
- Reduced hopper reentrainment
- Increased agglomeration of fine particles

A flue gas conditioning system would have several advantages as a retrofit technology for ESPs. Because it would require no modifications to the ESP, it would be very cost effective. Flue gas conditioning systems that are currently available are relatively simple and can be applied to almost any ESP. The installation would require minimal downtime of the boiler. Finally, it could also be used on new ESP designs to provide high collection efficiency with a reduced collection area.

Program Objectives

The purpose of this research program is to identify and evaluate a variety of additives capable of increasing particle cohesion which could be used for improving collection efficiency in an ESP. A three-phase screening process will be used to provide the evaluation of many additives in a logical and cost-effective manner. The three step approach involves the following experimental setups:

1. Provide a preliminary screening in the laboratory by measuring the effects of various conditioning agents on reentrainment of flyash particles in an electric field operating at simulated flue gas conditions.
2. Evaluate the successful additives using a 100 acfm bench-scale ESP operating on actual flue gas.
3. Obtain the data required for scaling up the technology by testing the two or three most promising conditioning agents at the pilot scale.

Measures of Success

It is difficult to establish objective quantitative goals for the program that can be expressed in terms of a measurable improvement in performance. The nature of the difficulty in establishing measures of success lies in the problem being addressed in this program. The objective of the program is to investigate conditioning agents that will produce improved collection efficiency of fine particles in an electrostatic precipitator. However, the additives will not have any impact on the primary particle collection mechanisms which are well understood theoretically and are easy to experimentally verify. Instead, the additives will produce their desired effect by modifying only the non-ideal effects, and these are not associated with either solid fundamental understanding or specific measurement technologies.

The "non-ideal effects" represent, by definition, the mechanisms that cannot be explained by ESP theory but are a very real part of the performance of a full-scale ESP. The non-ideal effects fit into several categories which include:

- Sneakage
- Non-uniform distribution of gas flow
- Non-rapping reentrainment
- Rapping reentrainment
- Hopper reentrainment

Since the first two non-ideal effects are due to the gas flow characteristics which result from the physical configuration of the ESP, the additives cannot be expected to affect these processes. However, an additive that increases the cohesive characteristics of the particles could decrease the magnitude of all forms of reentrainment.

The magnitude of rapping reentrainment can be measured by comparing emissions with and without rapping. However, the other non-ideal effects are continuous processes and are therefore difficult to quantitatively characterize. By measuring emissions at the outlet of an ESP, it is not possible to determine whether the particles are penetrating the ESP because they have not been collected or because they have either been reentrained or have by-passed the active sections of the ESP. About the only possible means to determine the cause of emissions is to compare actual performance with theoretical performance and then attribute the difference to non-ideal effects. However, this technique can only be effective if the non-ideal effects result in a significant contribution to the total emissions.

The role that the non-ideal effects play in ESP performance vary from unit to unit, but in general, the greater the collection efficiency, the greater the impact of the non-ideal effects. For a high efficiency ESP (i.e. 99.9% collection efficiency), non-ideal effects can be the root cause of the majority of emissions. Therefore, a process that reduces reentrainment will result in a large reduction in emissions. However, for a smaller and subsequently less efficient ESP, a similar reduction in the magnitude of reentrainment will have a lesser impact on overall emissions. For these reasons, any definition of a measure of success will have to take into consideration the size and performance of the ESP.

Another difficulty in defining a measure of success results from interpreting data obtained from reduced-scale precipitators. Although the additives have the potential for reducing all forms of reentrainment, rapping reentrainment and hopper boil-up cannot be adequately simulated in the bench-scale ESP. The primary effect of the additives that will be characterized in these tests will be non-rapping reentrainment. In the pilot-scale tests, rapping and hopper reentrainment will begin to become a factor, but because the plate height in the pilot unit is much smaller than full-scale plates, the magnitude of the effects of these forms of reentrainment will not be as significant. Therefore, a small improvement produced in the bench-scale and pilot-scale tests should represent the potential for a much greater amount of improvement when the additive is used in a full-scale unit.

Another major uncertainty is due to the fact that the ultimate target for this technology is not adequately defined at this point in time. The additives will be used as a retrofit technology on existing ESPs. The need for improving the performance of an existing ESP will be driven by either local regulations requiring a decrease in emissions or new regulations related to air toxics imposed at the national level. Since these specific standards will not be established until some time in the next couple of years, assumptions must be made about the specific targets for this program.

The final uncertainty is due to the site specific nature of the benefits of this technology. The relative reduction in outlet emissions produced by the additives increases with ESP efficiency. However, the lower the baseline efficiency, the greater the improvements have to be to meet a fixed standard. Therefore, there will be an optimum size ESP for this technology which will depend on the new regulations. If an ESP is very small, there may not be sufficient improvement available with the additives to reach the emission limits. On the other hand, very large ESPs may not need any improvement at all.

The age of the boiler might also play an important role in determining the cost-effectiveness of the additives. If there are many years of life left on a boiler, there might be justification of a large capital expenditure for a baghouse or new ESP. However, for a very old boiler with only a fews years of service remaining, the low-capital costs associated with chemical conditioning might appear relatively attractive.

Background

To understand how resistivity relates to particle reentrainment, it is necessary to understand how the different forces in the dust layer interact. In the dust layer on the collector plate, a surface charge density, σ, is created on the surface due to a discontinuity between the electric field, E_g, at the surface of the layer due to the corona wire voltage, and the electric field, E_l, created by the ionic charges on the collected particles. This charge density can be calculated by:

$$\sigma = \epsilon_0(E_g - \epsilon_l \rho_l J_p) \quad (C/m) \tag{1}$$

where ϵ_0 is the dielectric constant of free space and ϵ_l is the relative dielectric constant of the layer, ρ_l is the layer resistivity in ohm-m, and J_p is the current density. Equation (1) shows the surface charge density can be either positive or negative depending upon the electrical and layer conditions.

An electric force per unit area f_x acts on the surface charge

$$f_x = \sigma(E_g + E_l)/2 \quad (N/m^2) \tag{2}$$

The force f_x tends to pull the particles off the surface of the layer back into the gas if σ is positive. If σ is negative, the force tends to hold the layer against the plate.

Figure II-1 is a plot of the electrostatic force on the dust layer as a function of resistivity and the electric field strength at the plate. The calculations were made for a constant current density of 60 nA/cm^2 which is typical for a full-scale ESP. This family of curves demonstrates the general trends of the relationships defined by Equations 1 and 2.

When the resistivity is greater than 10^{10} ohm-cm, the electrostatic force rapidly increases toward the plate (i.e. increased clamping force) as the resistivity decreases. At these resistivity levels, the force is independent of the electric field at the plate and only a function of the product of the current density and particle resistivity. For high resistivity applications (i.e. $> 10^{11}$ ohm-cm) the holding force is so great that "power off" rapping is often required to remove the dust from the plates.

At particle resistivity levels below 6×10^9 ohm-cm, the electrostatic forces reverse and tend to pull the particles off the plates.

As can be seen from Figure II-1, for very low-resistivity levels, the repulsion force becomes relatively independent of resistivity, and correspondingly current density, and only proportional to the square of the electric field strength. Therefore, reentrainment in ESPs will primarily be associated with flue gases where sufficient SO_3 is available to reduce the resistivity below 10^{10} ohm-cm.

There are two additives that are in current use on a commercial basis to enhance the performance of ESPs. These are NH_3 and SO_3, which are used independently and together to improve the collection efficiency. The improvement is believed to be due mainly to changes in the electrical properties of the flyash, although there may be some increase in the adhesion of the particles from the agents.

The injection of NH_3 and SO_3 provides several physical and chemical effects that affect ESP performance:

- It can form solid ammonium sulfate, $(NH_4)_2SO_4$, particles which are very small and can increase the particulate space charge in an ESP and alter the electrical operating conditions.

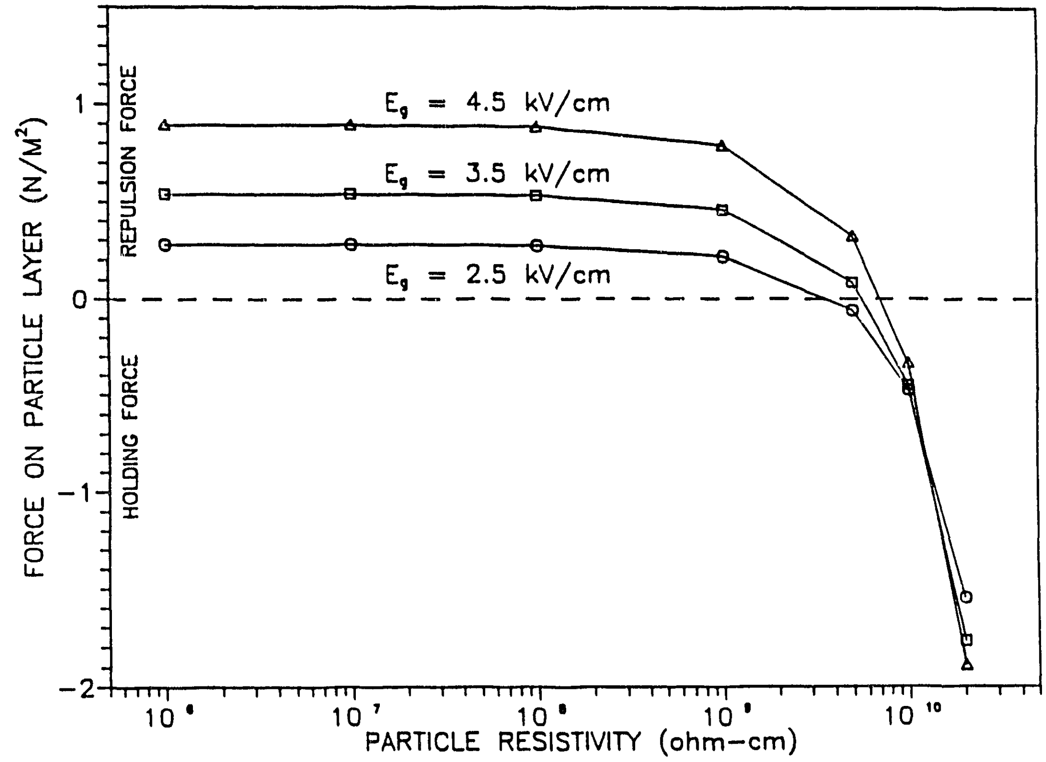

Figure II-1. Electrostatic Forces on a Dust Layer in an ESP.

- It can form liquid ammonium bisulfate, NH_4HSO_4 which condenses on the particles and increases their surface adhesion.
- It can modify the particle resistivity.

Whether ammonium sulfate or bisulfate is formed depends upon the flue gas characteristics and especially on the ratio of NH_3 to SO_3. Therefore, when testing with NH_3/SO_3 conditioning, the ratio of the two chemicals becomes an important parameter. However, in cases where the SO_3 is generated in the combustion process, as opposed to being injected, it becomes very difficult to control the ratio of the gases.

For conditioning with NH_3, there are two ways to inject the ammonia into the flue gas: vaporize anhydrous ammonia and inject it as a gas or inject a liquid chemical such as ammonium nitrate which will decompose in the flue gas to form NH_3. Since the end product of the conditioning in both cases is to supply NH_3 for reacting with SO_3, these two technologies will not be tested separately in this program. The differences between these two approaches only becomes important when comparing capital and operating costs.

III. Selection of Additives

The first technical task was to identify additives that could be injected into the flue gas to serve as an adhesive or wetting agent which would bind the fine particles together and thereby improve their collection in the ESP. In order to provide a more thorough coverage of potential conditioning agents, the search included products that were not specifically designed for ESPs. The major requirements of low toxicity and temperature stability were specifically noted. These products were reviewed to determine which ones are likely to survive and function in a flue gas at 300°F.

Candidate additives covered a range of chemicals and include surfactants, adhesives, polymer resins, foams, and emulsions. The following paragraphs describe classes of materials that were evaluated during this program.

These compounds are:

- Starches
- Gums
- Cellulose Derivatives
- Vegetable Oils
- Waxes
- Mineral Oil
- Polyacrylamide
- Poly(ethylene glycol)
- Poly(propylene glycol)
- Polyvinylpyrrolidone
- Vinyl Alcohol Polymers
- Acrylics

Starches

Starch is a natural polymer consisting of glucose units chemically bound together to form a nonrecurring polyhydroxy material. Starch granules consist of para-crystalline solids, and range in size from 1 to 100 microns. Most of the starch used in the U.S. is produced from corn, *Zea mays*, and consists of amylose and amylopectin. Amylose is a straight chain molecule utilizing 1,4 linkages. Amylopectin is a branched molecule utilizing 1,4 and 1,6 linkages.

Starch-based adhesives are used in papermaking, paper coating, corrugating, bag adhesives, laminating adhesives, tube winding, case sealing adhesive, gummed tapes, label and envelope adhesives, textiles, wall covering adhesives, and various other applications. In 1980, 5% of the U.S. production of corn (21 X 10^6 m^3 or 6 X 10^8 bushels) was ground for starch.

Waxy Corn Starch

Waxy corn starch contains only amylopectin. It is water soluble, and due to the high amylopectin content, tends to form weak, water sensitive films. Waxy corn starch is the basis for jelly gums, which are used in bottle labeling. Waxy corn starch is non-toxic, and can be used as a food additive or as an adhesive. The cost of waxy corn starch in bulk quantities is \$0.44/lb.

Corn Starch

Regular corn starch contains 72% amylopectin and 28% amylose. It is water soluble, non-toxic, and is a food additive. Corn starch must be heated or alkali treated to release starch molecules from granules. The price of bulk corn starch is \$0.14/lb in truckload quantities. Treating corn starch with a solution of 0.8% sodium hydroxide (w/w) creates a more viscous mixture which does not crystallize as readily on cooling as is the case with non-treated corn starch.

Corn Syrup

Corn syrup is produced from the partial hydrolysis of corn starch into dextrose, maltose and higher molecular weight saccharides. It is a clear, colorless, viscous liquid. The price of corn syrup is \$0.15/lb in truckload quantities.

Dextrins

Dextrins, or starch gums, are derived from starch. Dextrins have high affinity for polar compounds such as water due to the large number of hydroxyl groups on the chain. The process of dextrinization, a type of hydrolysis, is accomplished using dry heat in the presence of acids. Depending upon the temperature and amount of acid used, several types of dextrins are formed. In general, all dextrins are water soluble and non-toxic. Dextrins are used widely as adhesives in food packaging.

A selection of dextrin-based adhesives were be obtained from Swift Adhesives. Temperature, strength, and viscosity can be adapted for specific applications.

White Dextrin - White dextrins are prepared by heating starch and large amounts of acid to 258°F for 3-7 hrs. The color is white to cream, and the solubility and viscosity varies. They are used in tube winding, case and carton sealing, laminating, gummed sheets, label and envelope back seam adhesives. The current price is $0.36/lb.

Canary Dextrin - Canary dextrins are prepared by heating starch and moderate amounts of acid to 300°F for 11 hrs. They are very light to dark tan in color, have a high cold water solubility and a low viscosity. They are used in gummed tape, envelope front seals, stamps, case and carton sealing, laminating and tube winding. The current price is $0.36/lb.

British Gums - British gums are prepared by heating starch with a low amount of acid at 330°F for 17 hrs. They are dark in color and have varying solubilities and varying viscosities. They are used solid fiber laminating, bag-seam pastes and tube winding adhesive.

Gums

Gums are hydrophilic polysaccharides derived from plants or microorganisms which produce viscous mixtures or solutions. Natural gums are carbohydrate in nature, and vary considerably in the details of their chemical structure. Technically, natural gums include starches and celluloses, but they are considered separately in this discussion.

Natural gums include plant exudates (gum arabic), seed gums (guar gum, locust bean gum), plant extracts, seaweed extracts (agar, carrageenan) and the extracellular microbial polysaccharides (xanthan gum). These natural gums are harvested and produced in an organized way by the chemical industry, so are available in a variety of grades. Gums are used in detergent and laundry products, textiles, adhesives, paper, paint, food, pharmaceutical and cosmetics industries.

Gum Arabic

Gum arabic is an exudate from the acacia tree. It forms as 'tear drops' of exudate from wounds in the bark of the tree. It is a branched polymer of galactose, rhamnose, arabinose and glucoronic acid. Gum arabic usually contains calcium, magnesium and potassium salts, and has a molecular weight of 250,000 to 300,000. Gum arabic is very soluble in cold water, and its solutions have a very low viscosity. These solutions have distinct adhesive properties.

Gum arabic is used in the food and pharmaceutical industries where it is used as an edible binder. It is also used in lithographic printing as a light-sensitive coating when mixed with potassium dichromate. It is non-toxic, although it can possibly act as a weak allergen. The price of bulk gum arabic is $5.00/lb.

Locust Bean Gum (Carob Bean Gum)

Locust bean gum is derived from seeds of the tree *Ceratonia siliqua*. The tree takes 5-10 years to produce seeds. The endosperm of the seed is the source of the gum and is separated from the seed coat and embryo by milling. The endosperm is then ground and graded according to size, color, etc. Food grade locust bean gum typically contains 80% gum, and is white to yellowish-white, odorless powder. Locust bean gum is a galactomannan polysaccharide, which is a straight chain polymer of mannose with one galactose branch on every fourth mannose. The molecular weight of the gum molecule itself is reported at 310,000.

Locust bean gum is partly soluble in cold water, but completely soluble in hot water. Maximum viscosity of the heated solution is obtained upon cooling. It is nonionic in character, and gels can be formed with alkaline borates or mixing with carrageenan extract.

Locust bean gum is used in the food, papermaking, textile sizing and printing, and cosmetics industries. It is non-toxic, and is used as a stabilizer food additive and thickener. Locust bean gum is not digested by animals.

Annual production of locust bean gum in the U.S. is around 2,000 tons. World-wide production is an additional 3,000 tons. The price of bulk food-grade locust bean gum is $4.00/lb, and can be obtained from Rhone-Poulenc.

Guar Gum

Guar gum is an extract from the seeds of *Cyanopsis tetragonolubus*, a leguminous plant cultivated in Pakistan, India and Southwest United States. The extracted gum consists of a mannose polymer with galactose branches on every 2nd unit. This makes it very similar to locust bean gum. It is soluble in cold water, and the solutions have a high viscosity. Some commercial guar gum products have a slight degree of chemical modification to improve solubility in cold water or other properties. Rhone-Poulenc produces guar gum with various types of modifications.

Guar gum is used in the same way as locust bean gum, but supplies of guar gum are more regular and reliable, and also cheaper. Guar gum is not as heat tolerant as Locust bean gum or Xanthan gum. It is used in the food, papermaking, mining, and petroleum industries. It is a non-toxic, stabilizer food additive and thickening agent. The price of unmodified guar gum is $2.50/lb in bulk quantities.

Carrageenan (Vegetable Gelatin)

Carrageenan is an extract from Irish moss, the red seaweed *Chondrus crispus*. It contains two main polymeric fractions; kappa-carrageenan and gamma-carrageenan. Both are sulfated polysaccharides (anhydrogalactose-galactose polymer sulfate ester). Carrageenan is soluble in water, forming viscous solutions.

Carrageenan is used in the pharmaceutical and cosmetics industries. It is used extensively in the food industry as a stabilizer food additive in many 'instant' foods. Pure carrageenan can be purchased from Sigma Chemical for $13.75/100g.

Algin (alginic acid, alginate)

Algin is the main carbohydrate polymer in brown seaweeds, especially *Macrocystis pyrifera, Laminaria and Ascophyllum nodosum*. Algin is a linear polymer of mannuronic and guluronic acids. Alginic acid is nearly insoluble in water but is strongly hydrophilic. Sodium alginate dissolves in cold water, making somewhat viscous solutions. Propylene glycol alginate is soluble in water and has distinct commercial importance. Alginate solutions have very good flow properties, which is why they are used in industrial applications.

The textile industry is the major user of alginates. Solutions of the gum can be adjusted in viscosity and flow properties to suit many kinds of printing machinery and fabric texture. Alginates are also used in medicine and as a food stabilizer. They are also used for paper coating, photographic and lithographic purposes.

Agar (Gum Agar)

Agar is an extract from the red seaweeds *Gelidium* and *Gracilaria*. Normal samples of agar contain more than one polymeric substance. The main polymer is agarose, which contains galactose alternating with units of 3:6-anhydrogalactose. The second component is called agaropectin, which contains some sulfate ester groups. Agar is insoluble in cold water, but readily soluble in boiling water. Upon cooling the solution remains liquid until about 40°C is reached, when the mass sets to a very strong gel. The gel does not melt again until about 95°C is achieved (temperature hysteresis).

Much of the agar produced is used in the food industry as a gelling agent and a stabilizer food additive. Agar is used in the dentistry, medicine and microbiology industries also. The price of bulk agar was $12.67-14.87/kg in 1979. Pure agar can be purchased from Sigma Chemical for $12.90/100g.

Xanthan Gum

Xanthan gum is an extracellular polysaccharide produced by fermentation of dextrose with *Xanthomonas campestris*. The polysaccharide is recovered from the fermentation solution by precipitation and purification with isopropyl alcohol, followed by drying and milling to yield commercial xanthan gum. It is an unusual polysaccharide polymer of glucose, mannose, potassium glucoronate, acetate and pyruvate. Xanthan gum is a very long, linear polymer with a molecular weight ranging from 1 million to 10 million.

Xanthan gum is soluble in cold or hot water and forms viscous, neutral, and nonthixotropic solutions. Xanthan gum solutions are unusually stable towards changes in temperature, acidity, alkalinity and salt content.

Xanthan gum is used in oil well drilling muds because of its heat stability and tolerance to salts. It is also used in certain textile dyeing systems. Xanthan gum is used as a stabilizer, thickener and an emulsifying agent in pharmaceutical and cosmetic applications. Purified xanthan gum is an approved food additive which serves as a stabilizer, emulsifier, thickener, suspending agent, bodying agent and foam enhancer.

The price of bulk xanthan gum is $4.00/lb to $4.50/lb and can be obtained from Rhone-Poulenc.

Cellulose Derivatives

Cellulose is the major chemical constituent of plants. It is a homogeneous polysaccharide formed from glucopyranose units linked together. It is a semicrystalline polymer, and cannot be melted before it burns.

Hemicellulose is a noncrystalline group of heterogeneous polysaccharides which are the second-most abundant source or carbohydrates in plants. They are located in the cell wall of plants and in the bast fibers of bark. Commercial production of cellulose derivatives is concentrated on the pure sources like cotton or easily harvested sources like wood.

Methylcellulose

Methylcellulose is a class of water soluble cellulose ethers derived from cellulose. They are used in foods, cosmetics, pharmaceuticals, latex paints, construction products, and ceramics. They are used as thickeners, binders, film formers, water retention agents, suspension aids, surfactants, lubricants, protective colloids and emulsifiers. One unusual characteristic of these compounds is the ability to thermally gel.

There are various types and grades of methylcelluloses, each having unique properties. The two types available from Dow Chemical Corp. are methylcellulose and hydroxypropyl methylcellulose. Both are made by the reaction of wood or cotton cellulose fibers with chemical reactants in the presence of a caustic soda. The product is then purified and ground into a fine powder. Methylcellulose is made using methyl chloride while hydroxypropyl methylcellulose is made using propylene oxide and methyl chloride.

Methylcelluloses are soluble in cold water, non-ionic, stable over a wide pH range, have little odor, and are metabolically inert. Aqueous solutions of methylcelluloses gel when heated above a particular temperature, then go back into solution upon cooling. The viscosity ranges from 3 to 100,000 mPa·for various types and grades.

Both types of premium cellulose derivatives are recognized as acceptable food additives by the U.S. Food and Drug Administration. Methylcellulose is considered Generally

Recognized As Safe by the FDA. Standard grades of the cellulose derivatives have more impurities and are not approved for use in foods, but can be used in food packaging.

The char temperature for methylcellulose is around 437°F. The bulk price for methylcellulose is \$3.53/lb from Dow Chemical Coatings and Resins Dept. Hydroxylpropyl methylcellulose is \$2.71/lb from Dow.

Sodium Carboxymethylcellulose

Sodium carboxymethylcellulose, or SCMC has a hydroxyl group of the glucose units of the cellulose polymer chain-reacted to form a carboxymethyl ether. Thus, the properties of SCMC vary with the degree of substitution. SCMC is supplied as a powder of white to light cream color, and is available in a number of grades and viscosity types for use in foods, pharmaceuticals, cosmetics and many other products.

SCMC is anionic in nature, is soluble in hot or cold water, and tolerates ethanol or acetone in solution. The films of SCMC are insoluble in oils, greases, and organic solvents. SCMC is compatible with many water soluble salts, gum arabic, hydroxyethylcellulose, carrageenan, methylcellulose, polyvinyl alcohol, starches, other water-soluble polymers, glycerin, glycols, detergents and other synthetic polymer latexes.

SCMC is the cellulose gum used on the largest scale. A large amount of inexpensive SCMC is used in the formulation of synthetic detergents. SCMC provides a variety of functions for aqueous systems including thickening, rheology control and binding. The textile industry uses SCMC as a size for warp threads and for thickening textile printing pastes. SCMC is used as an adhesive for wallpaper, for thickening oil well drilling muds, for manufacture of synthetic latex, and in lithographic printing. SCMC of high purity is widely approved as a food additive and stabilizer. SCMC is used in the food industry to stabilize emulsions, prevent undesirable crystal growth, develop bulk and consistency, thicken solutions, and bind water in materials. SCMC is used in the pharmaceutical industry as a thickener, suspender, stabilizer and film-former for lotions, jellies, ointments and tablets. It is a stabilizer and thickener in cosmetics, an emollient in hand creams and lotions, and a foam stabilizer in bubble bath formulas (from Aqualon product information).

The char temperature of SCMC is 486°F. The price of bulk industrial grade SCMC is \$1.83-1.98/lb and can be obtained from Hercules Corporation under the name Aqualon.

Vegetable Oils

Most oils and fats are composed of a group of closely related compounds, the triglycerides. Triglycerides are formed by the reaction of the trihydric alcohol glycerol and fatty acids. Most of the fatty acids in natural oils occur as straight chains containing 12 to 18 carbon atoms. A few shorter chain acids are found in milk fats, while longer chains are found in certain types of fish oils. The properties of oils and fats are due to the properties of the component glycerides and their fatty acids.

Soybean Oil

Soybean oil is derived from the seeds of *Glycine max*. This is a leguminous plant native to China, but cultivated widely in the U.S. Crude soybean oil contains high levels of phosphatides (lecithin) and is greenish yellow in color. Refined and deodorized soybean oil is used for all edible purposes but does not give as good results as the other liquid oils such as corn oil. Large amounts of soybean oil are hydrogenated to form the basis of margarine, shortening, and other cooking fats. Soybean oil has a flash point 540°F. The bulk price of soybean oil is $0.65/lb.

Castor Oil

Castor oil is obtained from the seeds of the castor plant *Ricinus communis*. Castor oil differs from other vegetable oils in that its main component fatty acid is a hydroxy acid, ricinoleic acid. This gives the oil a high viscosity and specific gravity. Castor oil is used in medicine, cosmetics, as a lubricant or as a plasticizer for nitrocellulose lacquers. Modified castor oils are used in other industrial applications. Castor oil is also used in making nylon-11 and polyurethanes. The flash point of castor oil is 445°F. The price for bulk castor oil $0.85/lb.

Waxes

Carnauba Wax (Palm Wax)

Carnauba wax occurs as a fine powder on the leaves of certain tropical palm trees, especially *Copernicia cerifera*. The leaves are removed from the tree, dried in the sun, and then the powdery wax is brushed off and placed in vats of boiling water. The wax is then skimmed off the vat and treated further. There are various grades of carnauba wax. Carnauba wax is amorphous, hard, lustrous, and has a pleasing odor. It is a mixture of hydrocarbons, higher alcohols and their esters.

Carnauba wax is used in candles, polishes, lubricants, greases, floor and automobile waxes, insulating materials, soaps, salves, plastics, cosmetics, protective coatings and paper coating. It has low toxicity, and is a general purpose food additive. Carnauba wax has a flash point 540°F, and a melting point 185°F. The price of bulk carnauba wax is $1.25/lb.

Paraffin Wax (Petroleum Wax)

Paraffin wax is a white, translucent, tasteless and odorless solid. It consists of a mixture of solid hydrocarbons chiefly of the methane (paraffin) series obtained from petroleum. Paraffin wax is sold in various grades which differ from one another mostly on melting point. The largest percentage of paraffin wax sold is the refined type. The remainder is crude scale wax, which differs from refined wax in that it contains more oil (3%). This makes the wax softer and more crumbly, and the taste and odor are more noticeable. Paraffin wax has a flash point of 390°F, and an autoignition temperature of 883°F. Paraffin wax is an experimental carcinogen of the lung and stomach. Paraffin wax is produced by nearly all oil companies. The price for bulk paraffin wax is $0.50/lb.

Microcrystalline Wax

Microcrystalline wax is also derived from petroleum, but through a solvent extraction process, not distillation. It differs from refined paraffin wax in crystal size and structure. It is tougher, more flexible and has a higher tensile strength and melting point. Microcrystalline wax is also more adhesive and less lustrous and greasy than paraffin wax.

The oil content of microcrystalline wax varies with the grade of wax, but is usually 2-12%. The molecular weight of microcrystalline wax is 580-700, and contains straight chain molecules as well as a large proportion of branched-chain molecules. This accounts for the plasticity of microcrystalline wax when compared to paraffin wax.

Microcrystalline waxes usually melt at 145-195°F. The flash point >400°F. It has a low toxicity. Microcrystalline waxes are used in waterproofing paper, box-board, textiles, leather, wood, laminating paper, etc., rubber compounding, slushing compounds, polishes, paper making, binder for pipe coverings, filler for packings, drum linings, and vat linings. The bulk price is $1.00/lb.

Mineral Oil (Paraffin Oil)

A mixture of liquid hydrocarbons from petroleum. Flash pt.: 444°F. Inhalation of vapor or particulates can cause aspiration pneumonia. Mineral oils are recognized carcinogens of the skin and scrotum. Also experimental carcinogens of the larynx, lung and alimentary tracts. The bulk price is $0.52/lb.

Polyacrylamide

Polyacrylamide is a water soluble polymer used as a food additive. It has a low toxicity, although the monomer is highly neurotoxic. Polyacrylamide gives off ammonia above 480°F. Polyacrylamide is used in water treatment, paper making, mineral processing, and enhanced oil recovery. The nonionic polymer costs $2.00/kg. Polyacrylamide is produced by Dow Chemical, Exxon, Betz, and American Cyanamid.

Poly(ethylene Glycol)

Poly(ethylene glycol), or PEG, is a polymer of ethylene oxide which can be represented by the general formula $HO(CH_2CH_2O)_nH$, where n represents the average number of ethylene oxide units. They are linear polymers containing two terminal primary hydroxyl groups. PEG is water soluble, non-toxic, and have little odor.

Variations in physical properties are due to molecular weight. As molecular weight increases, viscosity and freezing point increase while solubility decreases. Methoxypropylethylene glycol is produced by the addition of a terminal methyl group and a terminal primary hydroxyl group. Many of the physical properties of the MPEGs are similar to PEG.

PEG is used as both a direct and indirect food additive. It is also used in pharmaceutical industry as a tablet coating, and as a base for ointments, lotions, and suppositories. PEG is also used in the cosmetics/toiletries industry in products such as toothpaste, soap, dentifrices, cake makeup, cream rouge, shaving cream, hand lotion, suntan lotion, hair dressings and conditioners, mascara, bath oils, emollients, cosmetic and antiperspirant sticks, and skin cleaning paste. PEG is also used in the rubber industry as a mold release agent and lubricant, as a binder for ceramics, and in the paint, paper, metal fabrication, textiles, and electronics industries. The bulk price is $1.16/lb.

Poly(propylene Glycol)

Polypropylene glycols (PPG) are polymers of propylene oxide and can be represented by the general formula $HO(CH_2CH(CH_3)O)_nH$, where n is the average number of propylene oxide groups. PPG is a clear, viscous liquid with low pour points. Viscosity increases with molecular weight. The lower molecular weight PPGs are soluble in water at room temperature, while the higher molecular weight PPGs have limited solubility in water. Dow Chemical PPGs meet the requirements of the FDA indirect food additive regulations listed in the FDA/EPA Status Selection.

PPGs are used as antifoam agents, lubricants, hydraulic fluid lubricants, heat transfer fluids, cosmetics and dust adhesive fluids, which are applied to air filters, dust mops, dust cloths, etc. to pick up and hold soil particles. The bulk price is $0.94/lb.

Polyvinylpyrrolidone

Polyvinylpyrrolinone, or PVP, is a polymer which is highly soluble in water and many solvents, and readily forms complexes. It has a molecular weight of 10,000-40,000 for most commercial grades, a boiling point of 95°C and a melting point of 13.9°C. The viscosity of aqueous solutions of PVP is low compared with other polymers. It fulfills the function of a protective colloid in many cases. It can form films and shows a good adhesion on many materials.

PVP is non-toxic, and is used in the pharmaceutical industry as a synthetic blood serum, a binding agent for tablets, and as a complexor with drugs. The cosmetics industry uses PVP in hair sprays, shampoos, hair rinses, shaving soaps and lotions, creams and toothpastes. PVP is also used in the textile industry, as a clarifier for wine and beer, in soap, detergents, polishing agents, water-soluble adhesives and ink. It is also used as a food additive. PVP is essentially an inert material and is non-hazardous when inhaled.

The price of PVP is $4.56/lb. GAF Corporation is the only producer of PVP in the U.S. although BASF sells resin imported from Germany.

Vinyl Alcohol Polymers

Poly(vinyl alcohol) or PVA is a water soluble polyhydroxy polymer. It is produced by the hydrolysis of poly(vinyl acetate), and was discovered in 1924. PVA is an excellent adhesive and has low surface tension, high tensile strength and abrasion resistance. The physical properties of PVA depend to a great extent on the method of preparation, which includes the polymerization conditions of the parent poly(vinyl acetate) as well as the hydrolysis conditions, drying and grinding. The viscosities of PVA solutions are dependent on molecular weight, concentration, hydrolysis and temperature. The surface tension of aqueous solutions of PVA varies with concentration, temperature, degree of hydrolysis and acetate distribution on the PVA backbone.

PVA is a nonhazardous material according to the American Standard for Precautionary Labeling of Hazardous Industrial Chemicals. It has a low oral toxicity rating (rats), and low toxicity in bluegill sunfish at concentrations of 10,000 mg/l in water. Short-term inhalation of PVA dust has no known health significance but can cause discomfort and should be avoided as a one would a nuisance dust. PVA is also one of the few completely biodegradable synthetic polymers when treated with an activated sludge.

The main uses of PVA are in fibers, adhesives, emulsion polymerization, production of poly(vinyl butyral), and textile and paper sizing. Other uses are as joint cements for building construction, water-soluble films for hospital laundry bags, emulsifiers in cosmetics, solid binding for erosion control, and cold water-soluble packaging for pesticides, herbicides and fertilizers.

The principal PVA producers are Air Products and Chemicals, Inc. and DuPont. The price has historically reflected the cost of ethylene, acetic acid, and energy and currently costs $1.47/lb for bulk quantities.

Acrylics

Acrylic adhesives are based mainly on ethyl, butyl and 2-ethyl hexyl acrylate monomers, plus small quantities of methyl methacrylate and acrylic or methacrylic acids. Frequently the acrylic monomers are copolymerized with other vinyl monomers such as vinyl acetate, vinyl chloride, or styrene. This permits the synthesis of linear polymers of very high molecular weight. Water soluble polymers can be made through proper monomer and functional group selection. Emulsions of other, non-water soluble acrylics can also be made.

The viscosity of the polymer solutions increases directly with molecular weight. Acrylic adhesives have low toxicity and high water resistance. Acrylic polymers are widely used as adhesives for pressure sensitive tapes, labels, and other pressure sensitive products. Acrylics are also used in a variety of waterborne construction adhesives, laminating adhesives, and packaging adhesives.

IV. Initial Screening of Additives

The work plan called for a two-stage screening process for the additives to determine their ability to improve the collection of flyash particles in ESPs. The first test series was an investigation of the survival of the candidate additives and a qualitative evaluation of the mixture cohesivity at a temperature of 300°F, typical of flue gas duct conditions. In the second test series, materials that successfully completed the exposure testing were added to a simulated flue gas stream and their effect on flyash deposited in an electric field were evaluated.

This section describes the first phase of laboratory screening in which various polymers and natural compounds were tested in the laboratory for their suitability as ESP additives. Table IV-1 presents a list of the additives that were evaluated. Initial tests consisted of mixing 5 g of flyash with 5 ml of an aqueous additive solution. Additive solutions of both 0.1% and 1.0% were added in equal amounts to a flyash sample. This mixture was placed in an aluminum dish and weighed. The dish was then heated at 300°F for two hours, weighed, heated for an additional 3 hours and weighed again. The characteristics of the final heated samples were then inspected and subjectively judged relative to the cohesiveness of the dust cake. The observations were recorded and graded on a cohesive scale from + (low) to +++++ (high). The results are presented in Tables IV-2 and IV-3.

A visual portrayal of the effects of different additives is given in Figure IV-1. The Figure shows two different effects caused by additives. Additives believed to provide a beneficial cohesive effect produced large cementatious formations. Additives which were believed to be less effective produced either no visual difference in appearance or they formed extremely small cohesive particles. These visual observations formed the basis for the initial screening process.

At a concentration of 0.1% it was difficult to determine large variations between samples, so tests using 1.0% solutions were done. Most of the additives performed better at the higher concentrations, except for a few. All of the glycols and the Swift adhesives performed better at the lower concentrations. This may be due to interactions between the polymers and the ash particles.

Table IV-1. Additives Tested During Initial Laboratory Screening

Starches:	Waxy corn starch (amylopectin)
	Corn starch
	Corn syrup
	Dextrin adhesives (Swift adhesives)
Gums:	Gum arabic
	Locust bean gum
	Guar gum
	Hi-Tek guar gum
	Carrageenan
	Alginic acid
	Agar
	Xanthan gum
Polymers:	Poly(ethylene glycol) A
	Poly(ethylene glycol) B
	Poly(ethylene glycol) C
	Polyether polyol A
	Polyvinylpyrrolidone
Cellulose Derivatives:	Methylcellulose
	Sodium carboxymethylcellulose
	Hydroxypropyl methylcellulose
Oils:	Soybean oil
	Castor oil
	Mineral oil
Waxes:	Paraffin wax
Polyacrylamide:	Acrylamide/bis-acrylamide A
	Acrylamide/bis-acrylamide B

Table IV-2. Results of Initial Screening of Additives at a Concentration of 0.1%

Additive	Cake Characteristics	
Water Only	Brittle cake	0 cohesion
Carboxymethylcellulose	Brittle cake	++ cohesion
Methylcellulose	Brittle cake	++ cohesion
Hydroxypropyl methylcellulose	Brittle cake	+++ cohesion
Swift Adhesive A	Brittle cake	+ cohesion
Swift Adhesive B	Brittle cake	++ cohesion
Poly(ethylene glycol) A	Brittle cake	++ cohesion
Poly(ethylene glycol) B	Brittle cake	++ cohesion
Poly(ethylene glycol) C	Brittle cake	+ cohesion
Polyether polyol A	Brittle cake	+ cohesion
Polyacrylamide A	Brittle cake	++ cohesion
Polyacrylamide B	Crumbly cake	+ cohesion
Guar gum	Brittle cake	+ cohesion
Gum arabic	Brittle cake	++ cohesion
Amylopectin	Brittle cake	++ cohesion
Locust bean gum	Brittle cake	+++ cohesion
Hi-Tek guar gum	Brittle cake	++ cohesion
Carrageenan	Brittle cake	++ cohesion
Alginic acid	Brittle cake	+ cohesion
Agar	Brittle cake	++ cohesion
Xanthan gum	Brittle cake	+++ cohesion
Polyvinylpyrrolidone	Brittle cake	++ cohesion
Corn Starch	Brittle cake	++ cohesion
Corn Syrup	Brittle cake	+ cohesion
Soy Oil (1% detergent)	Brittle cake	+ cohesion
Castor Oil (1% det.)	Brittle cake	+ cohesion
Mineral Oil (1% det.)	Brittle cake	++ cohesion
Paraffin Wax (1% det.)	Brittle cake	+ cohesion

Table IV-3. Results of Initial Screening of Additives at a Concentration of 1.0%

Additive	Cake Characteristics	
Water	Brittle cake	+ cohesion
Carboxymethylcellulose	Brittle cake	+++++ cohesion
Methylcellulose	Brittle cake	+++++ cohesion
Hydroxypropyl methylcellulose	Brittle cake	+++++ cohesion
Swift Adhesive A	Crumbly cake	+ cohesion
Swift Adhesive B	Brittle cake	++ cohesion
Poly(ethylene glycol) A	Brittle cake	0 cohesion
Poly(ethylene glycol) B	Brittle cake	0 cohesion
Poly(ethylene glycol) B	Brittle cake	0 cohesion
Polyether polyol A	Brittle cake	0 cohesion
Polyacrylamide A	Brittle cake	0 cohesion
Polyacrylamide B	Brittle cake	++ cohesion
Guar gum	Brittle cake	+++++ cohesion
Gum arabic	Brittle cake	+++++ cohesion
Amylopectin	Brittle cake	+++++ cohesion
Locust bean gum	Brittle cake	+++++ cohesion
Hi-Tek guar gum	Brittle cake	++++ cohesion
Carrageenan	Brittle cake	+++++ cohesion
Alginic acid	Brittle cake	+++ cohesion
Agar	Brittle cake	+++++ cohesion
Xanthan gum	Brittle cake	++++ cohesion
Polyvinylpyrrolidone	Brittle cake	+++ cohesion
Corn Starch	Brittle cake	++++ cohesion
Corn Syrup	Brittle cake	+++ cohesion
Soy Oil (1% detergent)	Brittle cake	+++ cohesion
Castor Oil (1% det.)	Brittle cake	++ cohesion
Mineral Oil (1% det.)	Brittle cake	++ cohesion
Paraffin Wax (1% det.)	Brittle cake	++ cohesion

a. Low Cohesivity

b. High Cohesivity

Figure IV-1. Effect of Additives on the Visual Appearance of Flyash.

All of the cellulose derivatives performed very well at both concentrations. The gums also did well, with unmodified guar gum, gum arabic, locust bean gum, carrageenan and agar providing the best cohesion. The Hi-Tek modified guar gum did well, but not as good as the unmodified guar gum. Amylopectin performed slightly better than regular corn starch, but both did very well.

None of the oils or waxes performed as well as the gums or celluloses. It was required that a detergent be added to the solution to solubilize the oils and waxes.

V. Experimental Apparatus

A laboratory flue gas simulator and injection chamber is used to produce a conditioned flue gas sample for evaluation in the ADA Field Resistivity Apparatus. The system, shown schematically in Figure V-1, was designed to provide a 1 to 3 acfm flow of gas with the following constituents: 0-40 ppm SO_3; 0-4000 ppm SO_2; 0-500 ppm NO; 0-20% O_2; 0-12% H_2O; 0-15% CO_2; 0-85% N_2; and a particle loading of 0.5 to 8 gr/acf.

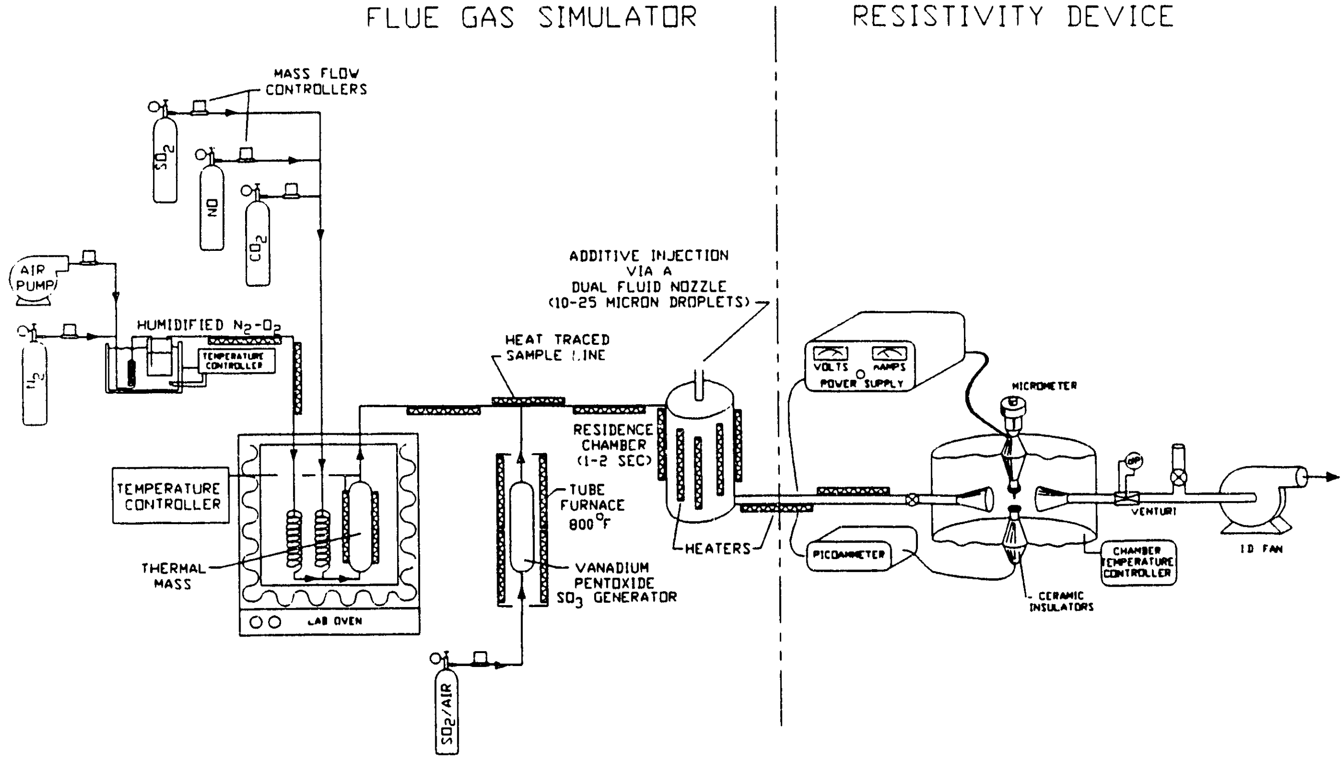

Figure V-1. Flue Gas Simulation System.

The dry gas phase constituents (NO, SO_2, and CO_2) were mixed and regulated using mass flow controllers and introduced into the heater/oven assembly. The mass flow controller units were individually calibrated for the particular gas against a bubble flow meter at 100% and 10% of full flow to assure the linearity and accuracy of the units. All of the gases were obtained as premixed certified standard compressed gases. The required N_2 and O_2 concentrations of the gas stream were produced through the dilution of room air with bottled N_2. This N_2-O_2 mixture was then passed through a temperature controlled water vaporizer to produce the necessary H_2O concentration. The vaporizer system was fully integrated in the flue gas simulation system with automatic controls. This allowed simpler operation of the system in a continuous mode. The humidified N_2-O_2 mixture was conveyed through heated sample lines to the heater/oven assembly where it was then mixed with the other gas constituents.

An electronic spread sheet was developed to compute operating parameters for the flue gas simulator system. The user inputs the desired composition and flow rate of the flue gas, the duration of the test, and the available cylinder concentrations of the individual gases. The spreadsheet then calculates individual mass flow controller settings, water vaporizer temperature, and gas volume (cylinder pressure) required to perform the test.

SO_3 Injection System

SO_3 is not available in gas cylinders, permeation tubes, or in any other pure, gaseous form (pure SO_3 crystals are readily available). Sulfan, which is a commercially available mixture of methyl alcohol (CH_3OH), methyl mercaptan (CH_3SH), and dimethyl sulfide (CH_3-S-CH_3) which decomposes in air to SO_3, CO_2, and H_2O, was considered as an option for the generation of SO_3. This option was ruled unacceptable due to health and safety concerns. The Occupational Safety and Health Administration (OSHA) 8 hour time weighted average (TWA) exposure limit for methyl mercaptan is 0.5 ppm and the potential for severe odor problems in a laboratory setting were the critical factors in this decision. Since SO_3 cannot be purchased in any pure form for use in gaseous mixtures, it was necessary to develop a reliable system for the generation of SO_3.

Utility flue gas conditioning systems and sulfuric acid (H_2SO_4) production plants utilize vanadium pentoxide (V_2O_5) catalysts to produce SO_3. The catalyst is kept at a temperature in excess of 800°F while a gas stream containing SO_2 and O_2 is passed through the bed. Within the catalyst bed the SO_2 is converted to SO_3 at an efficiency of 95% or greater. The bed does not require regeneration and no waste material is generated from the process. This type of system was chosen for the flue gas simulator due to its widespread use in industry, the ready availability of the catalyst, and the simplicity of the system.

Initial experiments were conducted using a laboratory grade, powdered catalyst containing 99.5% V_2O_5. The catalyst bed was formed by packing the powdered catalyst around glass beads in a stainless steel canister. The conversion efficiency of the bed was determined by measuring the amount of SO_2 upstream of the bed with the ADA Multigas Analyzer and then measuring SO_2 and total sulfate (wet chemical method for total sulfate) after the bed. Subtracting the SO_2 measurement from the total sulfate measurement yielded the SO_3 generation rate.

While this catalyst did generate SO_3, the generation rate was not stable and the conversion efficiency was poor (less than 75%) except when high concentrations of SO_2 were used (500 ppm or greater). Since the flue gas concentration of SO_3 produced from the combustion of a medium- to high-sulfur coal is between 5 and 20 ppm, numerous attempts were made to produce a consistent low concentration of SO_3 by varying the bed temperature (800 - 1000°F), increasing and decreasing the percentage of O_2 in the gas stream, diluting the gas stream with N_2, and removing the glass beads from the bed. All of these attempts to produce a consistent, low concentration SO_3 gas stream failed.

Since this catalyst was not capable of consistently producing low concentrations of SO_3 a sample of commercial catalyst used in sulfuric acid production plants was ordered. BASF's catalyst #04-111 did not require the use of the glass beads since it is manufactured as 6 mm long extruded pellets. The primary difference between this catalyst and the laboratory grade V_2O_5 is that the BASF catalyst contains only 95% V_2O_5 and trace amounts of sodium, potassium, and silica. The initial tests on this catalyst were not productive so the catalyst was left in the oven at a temperature of 950°F for 24 hours to determine if there was any effect to be gained from conditioning the catalyst at the desired operating temperature. After this conditioning period the catalyst was re-tested and was capable of producing a constant concentration of SO_3 down to 10 ppm at a conversion rate of almost 100%. The ADA Multigas Analyzer measured 10 ppm SO_2 at the inlet to the catalyst bed, 0 ppm SO_2 at the outlet of the catalyst bed, and the wet chemical measurements showed 12 ppm SO_3. While the SO_3 concentration was greater than the inlet SO_2 concentration it was within the margin of error for the aggregate calibrations of all the equipment involved.

Lower concentrations of SO_3 were not produced due to the limitations of the mass flow controller used to control the flow of SO_2 and due to the concentration of SO_2 in the gas cylinder. A 5000 actual cubic centimeter per minute (accm) flow head was installed and the flow rate to achieve 10 ppm was 3 accm. The accuracy of the flow controllers is decreased at both the high and low end of the range. The SO_2 concentration in the gas cylinder was 14,600 ppm. With a lower SO_2 concentration and a smaller mass flow controller head, lower concentrations of SO_3 could be produced in the flue gas simulator because the lower concentration required a higher flow rate which could be regulated more accurately by the mass flow controller.

After a consistent concentration of SO_3 was produced, experiments were conducted with flyash produced from the combustion of an eastern low-sulfur coal to determine the conditioning capabilities of the SO_3 injection system. The initial experiments involved placing a flyash sample in the ADA Resistivity Instrument, measuring the resistivity of the sample and then passing a simulated flue gas with 10 ppm of SO_3 through the instrument for 30 minutes. The particle resistivity was measured again after the 30 minute treatment time to determine the effect of the SO_3 conditioning. There was no significant change in resistivity over this time frame, so different methods of contacting the SO_3 and flyash were investigated. When this did not produce the desired effects, a thorough review of the literature revealed that it may take as long as 19 hours to produce a significant change in resistivity in laboratory experiments of this type. Long term conditioning tests were conducted which provided the SO_3 conditioning effects on particle resistivity that were expected.

Pre-screening tests were performed on the combined flue gas simulation-additive injection system to verify outlet humidity and SO_3 concentrations. Initial experiments indicated that the ash obtained from CONSOL was not responding to SO_3 conditioning. This is a very critical aspect of the laboratory experiments as the resistivity must be decreased to a level below mid-10^9 ohm-cm for particle reentrainment to become a limiting factor in ESP performance. If this level could not be achieved, then it would not be possible to detect an improvement when the additives are used to condition the ash.

The SO_3 was then mixed with the other flue gas constituents and injected into the resistivity device. A sample of ash was placed on the lower disc and the resistivity of the sample was measured. Initially the resistivity of the ash was in the range of 10^{11} to 10^{12} ohm-cm but after 10-12 hours of exposure to the simulated flue gas, the resistivity was reduced to 10^{10} ohm-cm. This long time delay has been reported for other laboratory evaluations on the effect of SO_3 on flyash resistivity (Bickelhaupt, 1978)*. It was assumed that this long conditioning time was due to the slow diffusion of gas through the 2 mm thick dust layer.

This long period for conditioning the ash was not be acceptable for the laboratory experiments with additives. However, when SO_3 is injected into actual flue gas where it mixes and interacts with flyash, there is only a one second residence time for the reduction in resistivity to occur. Therefore, the experimental system was designed to inject both flyash and SO_3 into a mixing chamber to provide at least a second of residence time for the gas to condition the particle. It was expected that this would provide a reasonable simulation of an actual conditioning environment. However, when the ash resistivity was measured with 5 to 10 ppm of SO_3 injected into the flue gas stream, no reduction in resistivity was detected and the resistivity remained in 10^{11}-10^{12} ohm-cm range.

Because of the time and expense of using the controlled condensation system to measure gas phase SO_3 concentration, a Land Dewpoint Meter was leased to measure changes in the acid dew point. The conditioning effect of SO_3 is due to an increase in the dew point from a water dew point, approximately 125°F for flue gas, to an elevated acid dew point, 250-300°F. Therefore, the presence of SO_3 in the flue gas exiting the resistivity chamber could be detected by the elevated dew point. However, the analyzer detected only the dew point due to water which indicated that the SO_3 had been scrubbed from the system.

Thermocouples were added to the flow system which identified the presence of several cold spots in the tubing. If the conditioned gas comes in contact with a cold wall, portions of the SO_3 will condense and not be available for conditioning the flyash downstream. In addition, some in-leakage was occurring through windows in the precipitator which diluted the relative SO_3 concentration.

The flow system was redesigned to solve the leakage problem and new heaters were installed to prevent cold spots. Additional temperature monitors were installed to continuously monitor the system. However, when the system was started up after the modifications, only minor reductions in resistivity could be detected when a relatively high concentration of 30

---

* Bickelhaupt, R.E. "Measure of Flyash Resistivity Using Simulated Flue Gas Environments," NTIS, PB-278 758, Southern Research Institute, Birmingham, Alabama, March 1978.

ppm SO_3 was injected. In addition, the unheated windows, which had a measured temperature of approximately 200°F, did not experience any fogging which indicated that the dew point was not elevated by the injection of SO_3.

Since the thermocouples confirmed that cold spots were eliminated, it was concluded that the ash was scrubbing the SO_3 from the flue gas. It is important to note that it is the gas phase SO_3 that leads to a lowering of resistivity and not SO_3 that has reacted on the surface of the flyash. Without the elevation of the dew point, there is no increase in the surface conduction on the flyash. Therefore, if the SO_3 does react with the flyash, there will be no elevation of the dew point and no decrease in resistivity.

Experiments were then run in which the injection rate for SO_3 was increased and the flyash injection rate was decreased. The purpose of these tests was to identify the condition that resulted in saturating the flyash with SO_3 such that gas phase SO_3 remained. It was discovered that indications of the presence of gas phase SO_3 could be detected when the flyash injection rate was reduced, such that the resulting inlet loading decreased from 2 to 1 gr/acf, with an SO_3 injection rate of 80 ppm. At this condition, the measured resistivity dropped to 10^8 ohm-cm and the windows on the precipitator began to fog.

Therefore, it was necessary to inject much higher levels of SO_3 in order to produce sufficient material to remain in the gas phase. This level is much higher than that found in actual flue gas. However, when SO_3 is measured in flue gas, the particles are in equilibrium with the gas and the SO_3 has already had a chance to react with the various flue gas constituents. It is not known how much SO_3 is generated originally in the boiler and subsequently removed through reaction with the surface of the flyash. Therefore, it is not unreasonable to assume that additional SO_3 must be injected into the simulated flue gas to equilibrate with the particles.

Additional tests were conducted to determine if the SO_3 injection rate could be increased to provide conditioning of higher concentrations of flyash particles. It was discovered that with the limitations of the flow controllers, 1 gr/acf was the highest concentration of particles that could be conditioned with the system. Therefore, tests were conducted at lower particle concentrations than originally planned.

Because of the interaction between the flyash and the injected SO_3, the plans for measuring reentrainment with and without the additives were modified. The original plan called for turning off the dust feeder during the reentrainment measurements. However, because of the interaction between the flyash and the SO_3, removing the particles would have resulted in a change in flue gas conditions. A new test procedure was devised to determine the impact of the additives.

By injecting high concentrations of SO_3 (80 to 100 ppm) it was possible to reduce the particle resistivity from 10^{11} to 10^7 ohm-cm. However, it was very difficult to consistently obtain intermediate levels of resistivity. This was because of the strong dependance between gas phase SO_3 and resistivity. It only takes a few ppm of SO_3 to provide an order of magnitude change in resistivity. This is demonstrated by the curves in Figure V-2. The water dew point for a gas stream with a moisture content of 10%, which is typical of coal fired boilers, is approximately 120°F. However, in a flue gas with only 2 ppm of SO_3, sulfuric acid will begin to condense at 270°F. The effect of the rapid rise in acid dew point is reflected by the corresponding rapid decrease in resistivity. With no gas phase SO_3 present, the resistivity is in the high 10^{11} ohm-cm range. However with only 10 ppm of SO_3, the resistivity drops three orders of magnitude. Therefore, intermediate levels of resistivity can only be obtained by controlling the SO_3 concentration to within 1 or 2 ppm.

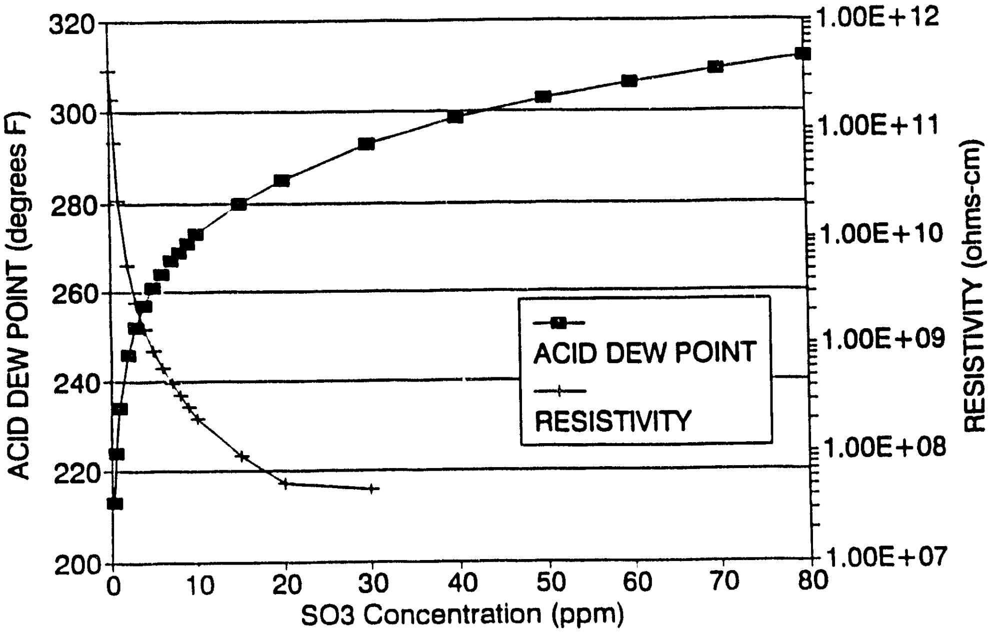

Figure V-2. SO_3 Dewpoint Temperatures.

Because of the fluctuation in the flyash feed rate and its impact on the gas phase SO_3 concentration, it was necessary to provide real-time feedback on actual SO_3 concentrations during the tests. Since there is no reliable continuous SO_3 analyzer manufactured, it was decided to design an acid dew point analyzer into the resistivity instrument, Figure V-3, by mounting a bare thermocouple on the inside of one window of the precipitation chamber. This window is located at the end of a pipe extending approximate three inches from the heated chamber. Since the window and pipe are unheated, the glass surface is cooler than the chamber. When the dew point temperature of the flue gas is higher than the glass temperature, a mist forms on the window. A heat gun is then used to heat up the glass from the outside. When the temperature of the glass rises above the flue gas dew point, the mist disappears. This temperature is recorded as the acid dew point. The measured acid dew point is then used to determine the SO_3 concentration from a calibration curve. This systems appeared to correlate well with the expected end result on particle resistivity.

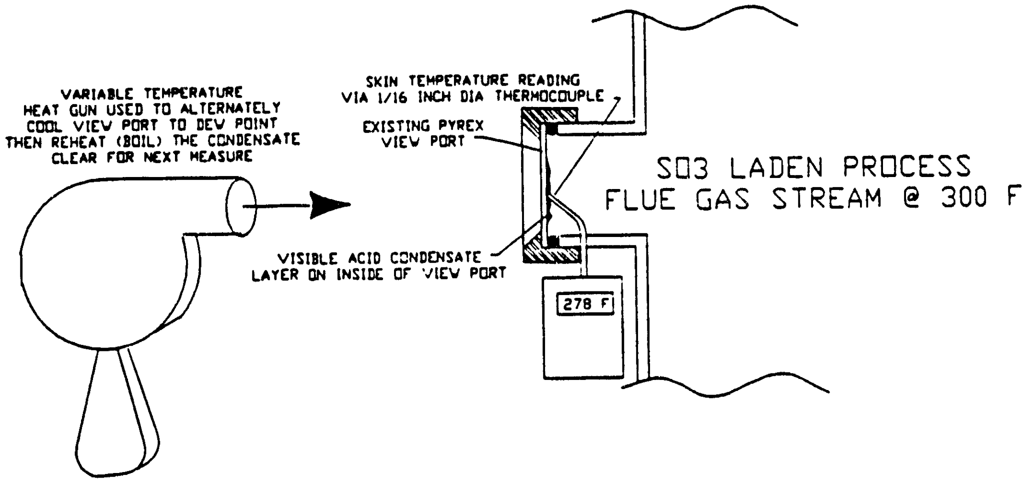

Figure V-3. ADA Resistivity Device Modified for SO_3 Dewpoint Measurements.

Figure V-4 shows a plot of measured SO_3, as determined by the acid dew point technique, versus the amount of SO_3 that was injected. With the injection of up to 30 ppm SO_3, there was no measurable change in flue gas conditions . However, at a feed rate of 80 ppm of SO_3, from 10 to 20 ppm of SO_3 could be detected in the gas stream. While injecting 140 ppm of SO_3, the dew point corresponded to 10 to 30 ppm SO_3. The variation in measured dew point at a constant SO_3 injection rate was possibly due to fluctuations in the flyash feed rate.

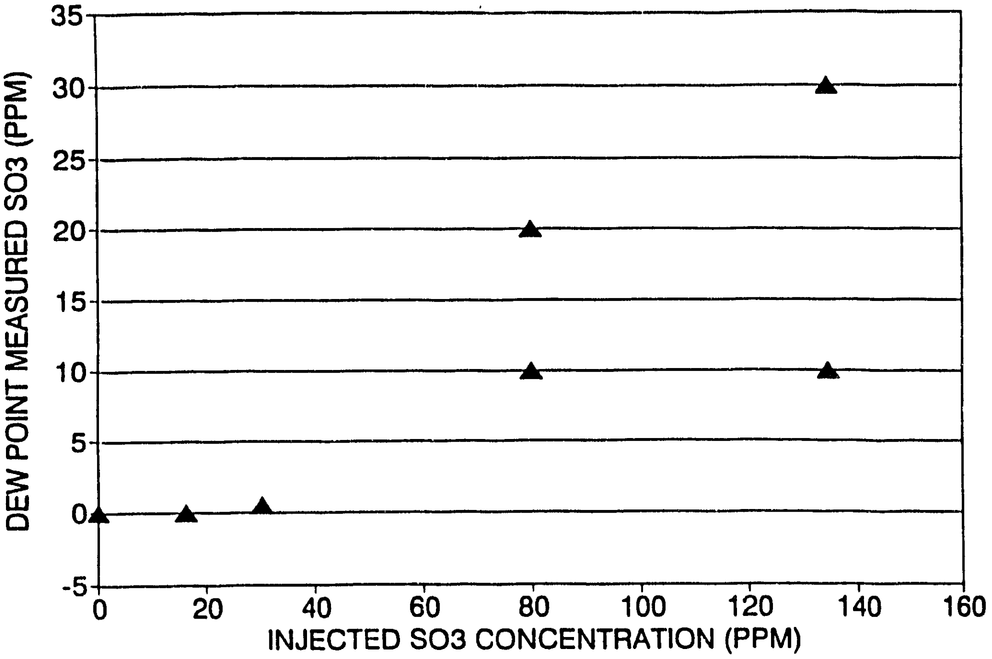

Figure V-4. Measured SO_3 Dewpoint Temperatures vs. Input SO_3 Concentrations.

A few tests were then conducted to see if collection efficiency in the resistivity instrument precipitator correlated with the resistivity measurements. Tests were conducted at three conditions representing 10^7, 10^9, and 10^{11} ohm-cm and are reported in Figure V-5. The precipitation rate was determined by measuring the precipitated dust layer thickness after a fixed sampling period.

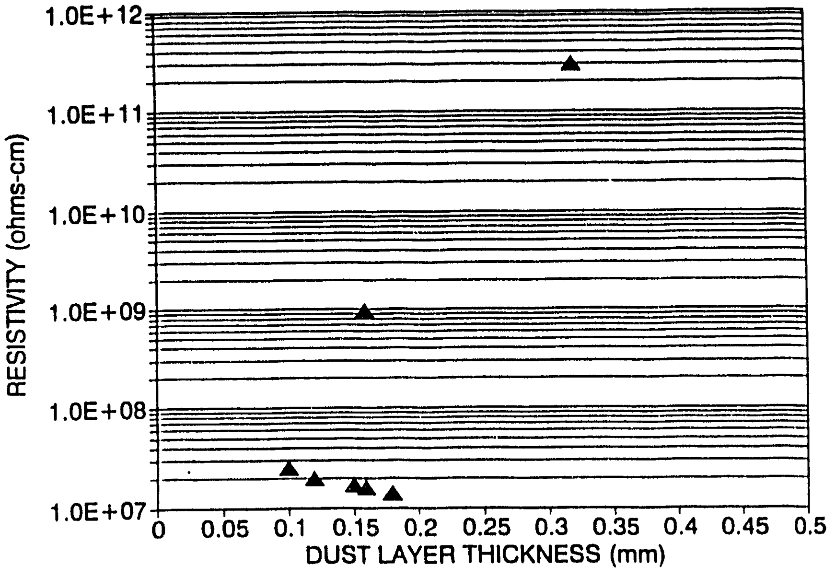

Figure V-5. Test Results Showing Flyash Precipitation Rates for Various Flyash Resistivities.

The precipitation rate for the 10^7 and 10^9 ohm-cm resistivity conditions were very low and were relatively equal. This is predicted by the relationships demonstrated in Figure V-2. However, the precipitation rate for the 10^{11} ohm-cm case was much higher. This indicates that the lower resistivity leads to increased reentrainment which limits the rate of precipitation. However, at a resistivity that is high enough to have a significant holding force on the collected particles, reentrainment is reduced and the dust builds up much faster. Since precipitation rate appeared to be a method of discriminating between two cases with different amounts of reentrainment, it was used as a criteria to judge the effectiveness of the additives.

It was very difficult to maintain experimental conditions that produced a consistent resistivity level of 10^9 ohm-cm. Therefore, it was concluded that the laboratory tests would be conducted at high levels of SO_3 such that the resulting resistivity was in the range of 10^7-10^8 ohm-cm.

There were several reasons leading to this conclusion. At SO_3 concentrations of 30 ppm and greater, the curves for both dew point and resistivity are relatively flat so that changes in gas phase SO_3 have minimal impact on particle characteristics. As shown in Figure V-2, electrostatic forces are relatively stable in this range so that changes in flue gas conditions that result in a change in resistivity by up to two orders of magnitude will have little impact on the magnitude of reentrainment.

Finally, at the very low resistivity conditions, reentrainment will be the highest. Since the purpose of the laboratory resistivity tests was to determine the relative ability of the various additives to reduce reentrainment, the greater the reentrainment, the easier it was to measure an improvement caused by an additive.

Design of Particle Injection System

A Vibra-screw mini dust feeder was sized and purchased to meter the flyash into the system. The unit is equipped with a DC motor drive so that the feed rate can be adjusted, and the feeder has been calibrated for flyash feed rates of 0 to 20 grains per minute. An eductor was sized and purchased to aspirate the particles from the output of the screw feeder and to mix them with the gases from the flue gas simulation system. Flyash samples were collected from the pilot ESP at the CONSOL Combustion Research Facility while burning a Western Kentucky 3% sulfur coal. This flyash was used as a standard for all of the screening tests.

Although the gas injection rate could be adjusted to accurately control SO_3 to within 1 ppm, the variation in the resulting concentration of gas phase SO_3 was greater that ± 10 to 20 ppm. Part of this variation was due to fluctuations in the screw feeder. At 1 gr/acf, the screw feeder must be operated in the lower ten percent of its capacity. At this rotation rate, the material inconsistently filled the flights of the screw. In addition, the calibration curve for the mass output of the screw feeder, Figure V-6, was very steep in the lower region so that a small change in setting produced a relatively large change in feed rate.

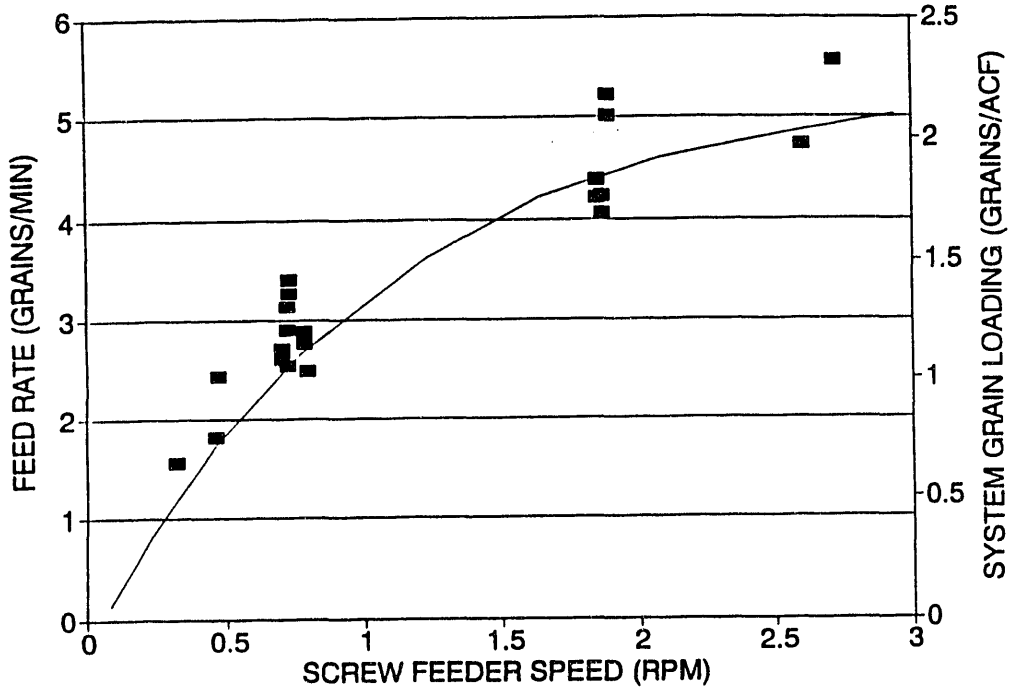

Figure V-6. Calibration of Flyash Feeder.

To overcome this problem, the screw was modified by adding a 0.035 inch diameter wire in the bottom of the screw flights as shown in Figure V-7. This filled up space that would have been filled with flyash during operation, so a higher rotation speed was required to produce a given mass flow. Although this reduced the magnitude of the fluctuation, it did not totally eliminate the problem so that it was still difficult to fine tune the SO_3 concentration.

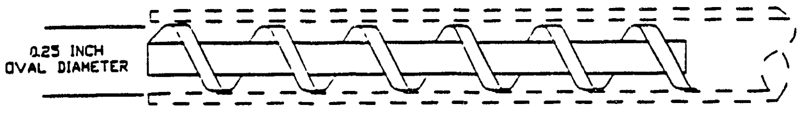

ORIGINAL SCREW IN SOLIDS FEEDER

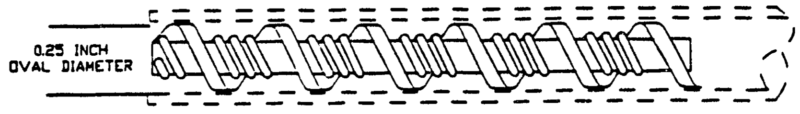

MODIFIED SCREW IN SOLIDS FEEDER

3 PASSES OF 0.035 INCH DIAMETER
STAINLESS STEEL WIRE BETWEEN THE
FLIGHTS TO REDUCE THE FLOW CAPACITY

Figure V-7. Modified Screw Flights of Flyash Feeder.

The laboratory flyash feeding system was modified to produce more consistent results. This was important because of the reaction between SO_3 and the flyash required maintaining a relatively constant ratio between the quantities of these materials being injected.

Variation of the flyash feed rate and plugging of the screw feeder even after modification to the supplied 1/4 inch diameter feed screw continued to present a problem with the laboratory apparatus. Another manufacturer of screw feeders was identified that produced 1/8 inch diameter single pitch feed screws. A 1/8 inch diameter feed screw was purchased and retrofitted into the screw feeder unit. Stirring whiskers or whips were also added in the solids hopper to prevent compaction of the flyash prior to feeding. A positive pressure purge of 15 standard cubic centimeters per minute of dry air was also plumbed into the solids feeder hopper to prevent any potential back flow of the simulated wet flue gas into the solids hopper were condensation might occur. The final modification to the screw feeder unit was the addition of a small electric solenoid rapper on the end of the feed tube where the flyash enters the simulated flue gas flow path. This rapper prevented the bridging of flyash clumps, promoting a more uniform feed rate.

These modifications to the solids feeder unit resulted in a significant improvement in flyash feed rate. Figure V-8 is a graph of the screw feeder calibration after retrofitting the 1/8 inch diameter feed screw. The screw feeder was operated at nominally 80 rotations per minute

(1/4 inch screw operated at 0.75 RPM) to provide approximately 3 grains per minute of feed. Control of the flyash feed rate became much finer and reasonably predictable. The flyash loading in the simulated flue gas mix entering the resistivity apparatus was visibly improved and more uniform.

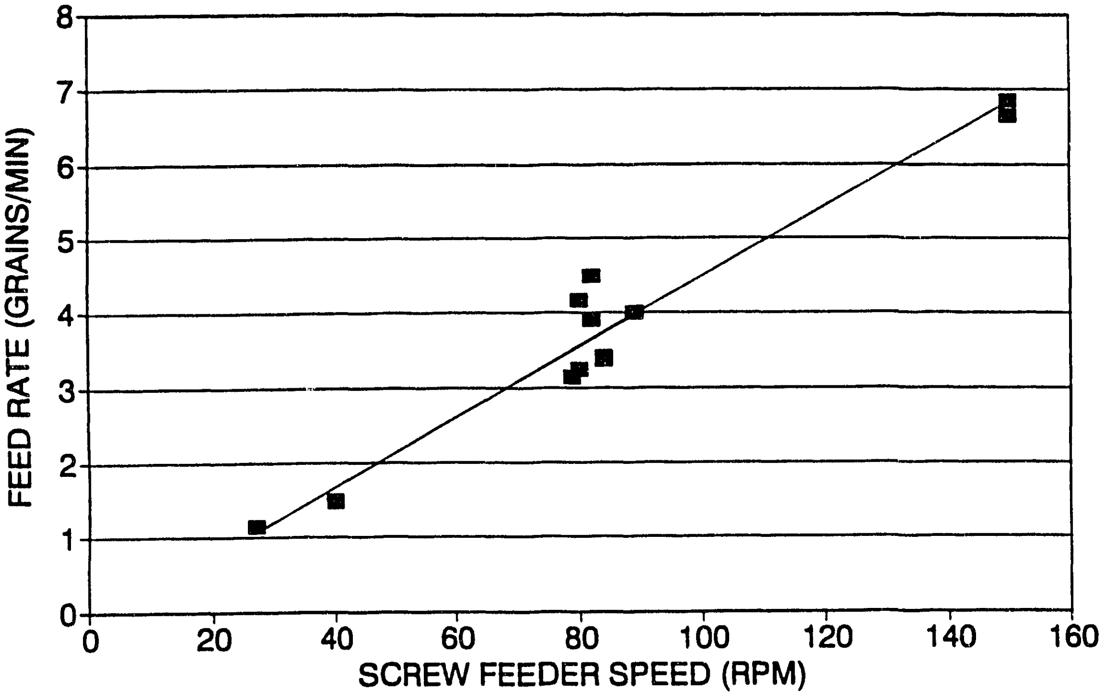

Figure V-8. Calibration of Flyash Feeder After Modification.

Additive Injection System

The additive injection chamber was designed for a minimum residence time of two seconds for flowing flue gas. The chamber is four inches in diameter and sixteen inches long. The bulk of the simulated flue gas stream enters the chamber tangentially. A slipstream of the flue gas is taken from upstream of the flyash feeder. This "clean" gas is introduced tangentially to an additive carrier stream flowing into the conditioning chamber from below. The positions of the two flue gas inlets produce a countercurrent swirl for effective mixing in the conditioning chamber.

For the laboratory tests, the additives were injected at very low rates, less than 0.1 gallon per hour. This eliminated most commercially available injection nozzles because they are designed for rates that are one to four orders of magnitude higher in flow. A review of several commercial nozzle catalogs did not reveal any nozzles that were viable candidates for the lab-scale hardware. The single technology that did appear to have promise was ultrasonic spray. One commercial system that sold for over five thousand dollars was briefly considered, but it was decided that it would be cheaper and quicker to test several candidate additives in an ultrasonic home humidifier.

To adapt the home humidifier to the lab-scale configuration, several modifications were made. The driver electronics and controls were removed from the humidifier housing in order to reduce its weight. This was needed in order to operate the ultrasonic transducer and supply tank while positioned on a digital balance so that the rate of mass loss in the supply tank could be measured and recorded. A separate injection tube was designed with a tangential inlet to add flue gas to the droplet spray so that a uniform flow of additive droplets could be injected into the contact chamber of the lab-scale setup.

The modified ultrasonic humidifier was tested in the ADA High Flow Test Bed facility to get a measure of the droplet size and velocity distribution generated. Tests were conducted for gum arabic, one of the candidate additives, at several dilutions and at two temperatures. Temperature is important because it directly affects the viscosity of the additive solution. A Phase Doppler Particle Analyzer (PDPA) was used to characterize the droplet size and velocity distributions from the ultrasonic humidifier. The PDPA is a point source measurement, so that to characterize the cross-section of a nozzle spray, several sample locations are investigated. The PDPA senses individual droplets, and can handle up to 50,000 droplets per second, a very dense spray.

A series of measurements was made on the vertical and horizontal bisector of the spray pattern. There was a very narrow distribution of droplet sizes measured in the tests. The Sauter mean diameter (SMD) measured for virtually all conditions was between five and seven microns. The Sauter mean diameter is an indicator of the diameter of the droplet population surveyed by the PDPA, and is calculated as the total volume of the measured droplets divided by the total surface area of those droplets. It is a valid indicator for processes that are surface-dominated, such as droplet evaporation. The five to seven micron value was found for all cases of liquid temperature, ultrasonic transducer amplitude, and additive dilutions tested.

A visual inspection of the injection tube indicated that the spray was uniform at the outlet, a condition which should promote good mixing with the incoming flyash-laden flue gas in the laboratory and bench-scale configurations. The measured velocities in the spray were found to average between one and one and one-half meters per second. Overall, the ultrasonic approach to the injection of additives to the simulated flue gas stream appears to be successful, and was employed in the laboratory testing.

Tests were conducted to determine how the additives would respond to atomization in the humidifier. The unit was filled with dilute solutions of several candidate additives and was found to produce a fine mist of small droplets. A test was run to determine the rate of droplet production in the unit, which included measurements made while varying the humidifier "rate control". The control appeared to regulate the amplitude of the sinusoidal driver voltage supplied to the ultrasonic transducer. Tests were run at the minimum and maximum settings for the control, which corresponded to 0.03 and 0.06 gallons per hour, respectively. These values were in the range of rates needed for the additive injection, depending on the final dilution and additive injection ratio used in the experimental hardware.

All additives were tested to determine the dilution ratios necessary for atomization with the lab scale additive injection system. The ultrasonic atomizer is not capable of atomizing most of the pure additives because of their high viscosity. These additives were diluted in water and atomized at room temperature and 180°F. The dilution ratio was chosen which required the least amount of carrier water for atomization.

The first several attempts at injecting additives into the simulated flue gas via the injection chamber revealed that the ultrasonic humidifier system was producing inadequately low liquid feed rates. The ultrasonic humidifier was characterized and calibrated previously in room air with several of the potential additives. A 1.5 inch diameter uptake tube similar to that used on the bottom of the injection chamber was used on these test. Use of the ultrasonic humidifier with the heated flue gas stream was expected to increase the feed rate due to increase liquid evaporation at higher temperatures. Several modifications were made in an attempt to increase the liquid feed rate of the ultrasonic humidifier with minimal success.

Under Task 4.2 - "Design of Additive Injection System", a dual fluid atomizing nozzle had been specified and ordered for use on the bench scale system and potentially the pilot scale system. The nozzle specifications show a minimum liquid flow capacity that was 1-2 orders of magnitude greater than what was need on the laboratory apparatus. Since modifications to the ultrasonic humidifier system were proving unsuccessful, a test of the bench-scale dual fluid nozzle was conducted to determine if it might be suitable for use on the laboratory apparatus.

A test of the nozzle was performed in which the minimum design atomizing air flow, 10,000 sccm (0.35 scfm), was supplied to the nozzle while the desired laboratory feed rate of liquid, 0.5 cc/min (0.008 GPH), was fed via a peristaltic pump. The minimum design liquid flow rate of the nozzle is 8.8 cc/min (0.14 GPH). The atomizing nozzle performs quite well at these extremely low liquid flow rates most likely as a result of the excessive amounts of atomization air. After visual and tactile examination of the spray plume the nozzle was inserted into the laboratory injection chamber. Complete evaporation of the injected liquid was occurring as there was no evidence of wall wetting or solids deposits in the main body of the injection chamber which has an inside diameter of 3.8 inches.

The gas mixing spreadsheet used for the laboratory flue gas simulator was modified to account for the 10,000 sccm of air injected into the chamber via the atomizing nozzle. The humidifier water bath temperature was adjusted accordingly to maintain the 10% moisture content desired as a baseline operation.

VI. Evaluation of Additives in a Simulated Flue Gas

Summary

Laboratory-scale testing involved injecting solutions of the different additives into a simulated flue gas and measuring the precipitated dust layer thickness in a point-plane precipitator. Additives used for this phase of testing were chosen based on the results of the screening tests described earlier. For each additive, testing was conducted by first operating at baseline conditions (no additives) and then repeating the test with additives. In order to produce gas stream characteristics which were identical under both baseline and additive conditions, the fluid injection nozzle was operated for both cases. During baseline testing, a 0.5 cc/min feed of clean water was injected through the nozzle into the contact chamber. A 250 ml flask acted as the reservoir for the peristaltic pump feeding the liquid. When testing an additive, a 250 ml flask containing the desired additive solution was exchanged "on the fly" with the baseline water flask. At the completion of an additives injection test, the process was reversed and a second baseline measurement was be performed. Tests were run for a constant duration. The data collected during each test included the resistivity of the precipitated material, the thickness of the collected dust layer, photographic documentation of the precipitated dust and subjective indications of the dust characteristics.

Several tests were repeated using the most promising additives. This was necessary due to the inconsistency in laboratory test conditions early in the program. By re-testing all of the best-performing additives after repeatable experimental conditions were achieved, a more sound basis for selecting the additives for the next round of testing was achieved. Tests were conducted on 8 types of additives. Four of these additives showed tremendous improvements in flyash precipitation rates.

Photographs presented in Figure VI-1 show an example of flyash precipitation rates observed during the laboratory-scale testing. A point-to-plane precipitator was used for these tests. Flyash precipitated under a baseline test condition (no additives) is shown on the left. The photograph on the right shows flyash precipitated under identical testing conditions with the addition of an additive. A significant improvement in the quantity of flyash collected during the additive test is visibly evident. Quantitative measurements of the thickness of the precipitated layers showed that four aditives produced significant improvements in precipitation rates compared to baseline tests.

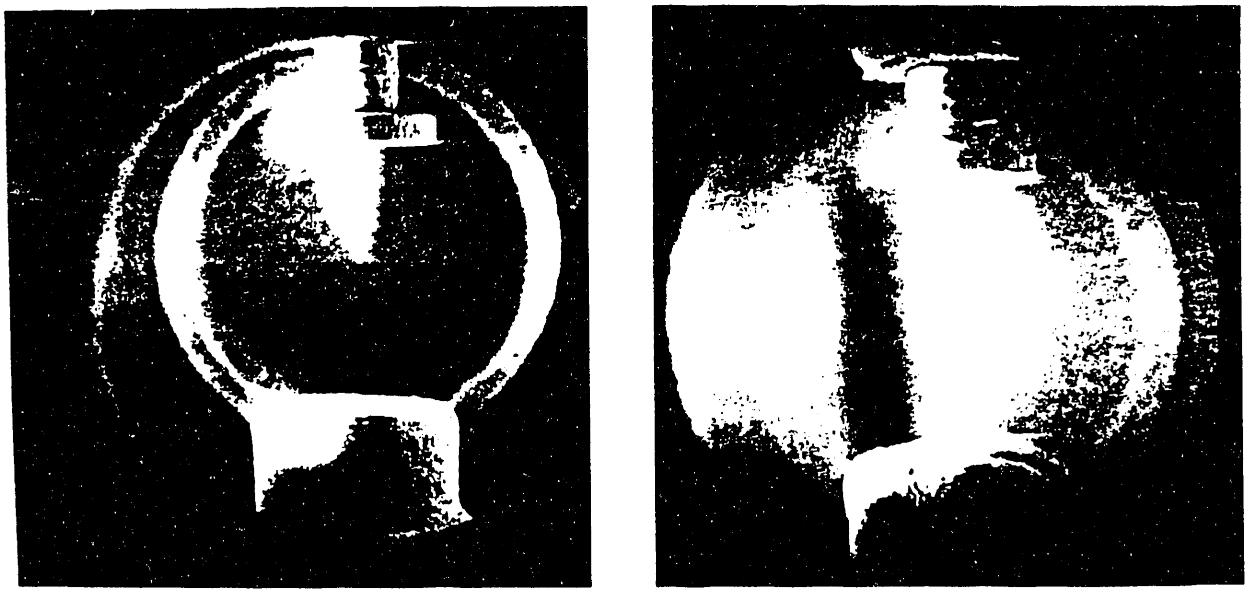

a. Baseline b. With Additives

Figure VI-1. Effect of Additives on the Characteristics of Precipitated Dust.

Figure VI-2 shows a graphical comparison of the performance of the most promising additives. The dark part of the boxes represents the thickness of the undisturbed precipitated layer, and the white part of the box represented the compacted thickness. The data are normalized so that the rate measured under baseline conditions represents unity. As can be seen, there were significant increases in the precipitation rate when the additives were injected.

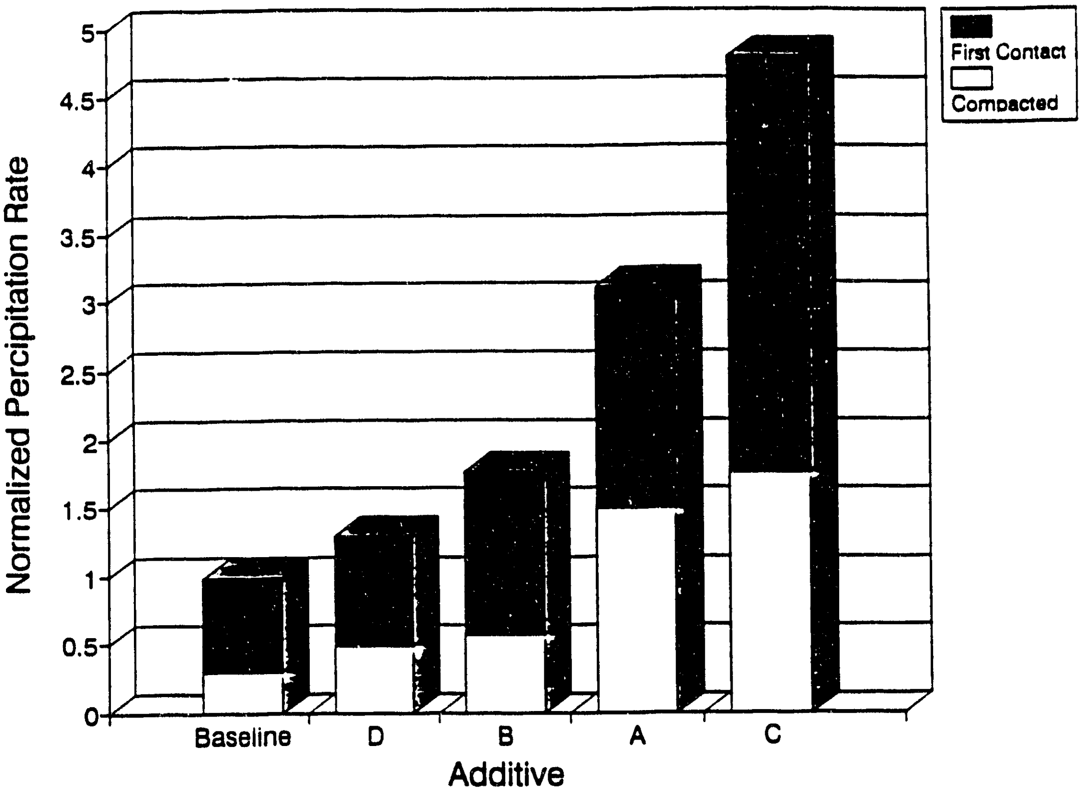

Figure VI-2. Comparison of the Precipitation Rates for Baseline Conditions and with Additives.

The additives shown in Figure VI-2 were added at a concentration of approximately 0.1% of the mass of the flyash in the flue gas. During the tests the gas stream characteristics, flow rate, particle resistivity, and ESP electrical conditions, were not affected by the addition of the additives. Therefore, it was concluded that the improved performance was due to increased particle cohesion. Because the precipitation disc is only a very small area compared to the volume of flow, even a minute increase in precipitation rate at this scale should result in a significant increase in efficiency in a full-scale ESP. However, with up to a five fold increase in precipitation rate in these tests, it is estimated that these additives have the potential to produce very large reductions in particle reentrainment.

The conclusion of increased cohesion is supported by changes in the physical characteristics of the ash as observed in photographs of the point-plane precipitator after a baseline test (flyash only and no additives) and after a test of the same duration and flyash feed rate with an additive injected (see Figure VI-1). The additive increased the thickness of the precipitated layer, which appears to be more "fluffy". In addition, there is a significant increase in the amount of material deposited onto the upper electrode. This indicates that the resulting flyash is indeed stickier.

The most successful candidates are non-toxic, as they are used in foods and cosmetic products. In addition, the chemicals are relative inexpensive. A very preliminary economic analysis indicates that the annual cost for additives for a 100 MW plant would be in the range of $10,000 to $100,000.

The additives fall into the general chemical category of natural polymers. These polymers are used in detergent and laundry products, textiles, adhesives, paper, paint, food, pharmaceutical and cosmetics industries.

Detailed Description of Laboratory-Scale Testing

The laboratory-scale testing was conducted in several phases in order to initially screen a number of additives and then to develop quantitative data on the best performing products.

The additives chosen for the first round of testing were diluted to the desired concentrations and refrigerated until use. A sample precipitation time of 20 minutes was selected for this series of tests. At the end of this period of time, the resistivity of the sample was measured. Subjective notes on the overall effectiveness of the additive were recorded to use for future comparison. In addition to the runs in which an additive was injected, baseline tests were conducted on a regular basis. The purpose of these runs was twofold: first, it served as a control standard which allowed a determination of inconsistencies in the system. Second, it became a reference point with which the relative effectiveness of the additive could be compared. The baseline runs were precipitated for the same amount of time as the injection runs and under identical conditions - the only difference being the injection of pure water through the nozzle rather than an additive. Due to the length of tubing and solution pumping rates, there was a delay time before the additive actually entered the additives chamber. To account for this delay, a time-out period of roughly thirty minutes was allowed between the start of injection and the precipitation test. Once this time had expired, the ESP was cleaned by removing the circular glass port and using a steel brush to remove the flyash that accumulated on the base, needle, and upper disc from the previous test. To finish the cleaning process, compressed air was blown on the contacting surfaces within the precipitation chamber.

Once the additive was in the system, the precipitation test was started. This involved bringing the high voltage supply to a point were the measured current was exactly 1.0 micro amps. To maintain this level, the voltage was monitored and adjusted as required. It was observed that as the flyash layer built up on the needle, a much higher voltage was required to maintain this current. During the precipitation time period, the following variables were documented:

Time
Voltage
Current
Sample temp
Skin temp
Air temp
Barometric pressure
Dew point

Following the precipitation test, the voltage was reduced to zero, and the upper disc in the resistivity device was lowered via a micrometer. In the initial testing of twenty additives, the disc was lowered until it would no longer move. This gave a measure of the thickness of the precipitated flyash. The resistivity of the flyash was then measured. The thickness of the sample (measured in mm) was used in a mathematical formula that calculates the resistivity of the sample. To formula for determining the resistivity of the sample is as follows:

$$\text{Bulk Resistivity} = (\text{Volts/Current}) * (\text{Area/Thickness}) \quad (\text{ohm-cm})$$

The twenty additives that were evaluated were ranked in order of effectiveness. The main criteria in this process was precipitation rate. However, several other criteria came into play. Since the system had many variables, and a variation in any one could affect the outcome of a test, it was important to account for the visual observations noted during each test. A prime example here is the solids feeder. Several times during the testing, the federate appeared to drop off dramatically. When this happened, one could logically expect the precipitation rate to decrease, so other test observations were relied on. Such was the case with Locust Bean Gum; During the initial test, the precipitation rate was just slightly better than baseline. However, it was recorded that the solids flow during the run was rather erratic, and the texture of the flyash appeared to be consistent with a well-performing cohesive material. Thus, this additive was recommended for a re-test over a longer precipitation time.

The top eight additives identified during the initial testing were selected for further evaluation. The objective for these test was to obtain more data in order to narrow down the list of additives that will be used during the bench-scale test. The following modification to the testing procedure was implemented: a precipitation time of one hour would be used. The reasoning behind the increased precipitation time was to limit the effect of uncontrolled fluctuations in the solids feed rate in hopes of improving data accuracy.

A change in hardware was also made for second round testing to include a test section (port) between the additives chamber and the resistivity device to allow for a "fret" test to be performed. This was designed to give an additional indication of the effectiveness of the additive. A fret made from perforated plate was placed physically in the gas flow entering the resistivity device. The fret occupied the entire cross section of the tubing carrying the gas flow. The thought was to weigh the fret before and after each test to give an indication of the amount of flyash sticking to a surface in the absence of an electrical field. However, this device had a tendency to plug within minutes and testing had to be terminated. This was the case with the Polyvinylpyrollodine test at a one percent concentration. As a consequence, the fret test was abandoned. .

A final modification to testing procedures included the taking of photographs during each tests in order to provide visual documentation of the results.

During this round of testing, a baseline test was run on a daily basis, and subjective notes were taken on all the runs. A total of ten baseline runs were conducted. The average precipitation rates were recorded and plotted. As expected, several additives performed much better than the baseline average. However, there were also some additives that had performed well in the original tests that actually resulted in a precipitation rate lower than baseline.

One explanation for this observation is the way in which the data were evaluated. The average baseline precipitation rate for the tests was calculated over a period of roughly two weeks. Therefore, any minor changes in flyash feed rate during a given test will impact the precipitation rate for that individual test. Since the additives were tested only once each per concentration over this time frame, the fluctuations in feed rate were not accounted for. As an example, the test of PVP at one percent concentration resulted in a precipitation rate of 0.28 mm/hr - just 0.06 mm/hr better than the baseline average. However, the two baseline tests conducted just prior to this test resulted in a precipitation rate of 0.155 mm/hr. Thus, compared to the baselines conducted at the same feed rate, PVP precipitated at a rate nearly twice that of baseline.

Also, comparisons between the two test series cannot be made directly. Since the first round of tests were conducted for only a twenty minute precipitation time, the results obtained may have been misleading in comparison to those obtained under different testing conditions during the second round of tests.

VII. Waste Characterization

A literature review was made to form a preliminary understanding of the characteristics of flyash containing conditioning additives based upon the following criteria: toxicity characteristics, handling properties, disposal properties and reuse capabilities. The review was based upon the chemical and physical properties of flyash and the proposed additives. Flyash samples will be collected during bench-scale and pilot-scale testing for actual chemical characterization for toxicity characteristics.

Toxicity Characteristics

Most coal combustion flyashes are characterized as "nonhazardous" according to the criteria established according to the U.S. Environmental Protection Agency's (EPA) Toxicity Characteristic. If the use of a conditioning additive raises the concentrations of regulated elements or organic compounds in Toxicity Characteristic Leaching Procedure (TCLP) leachates above regulatory levels, the leached material would be considered "hazardous". This would make disposal more difficult and costly.

The regulated elements and organic compounds should not be present in any of the proposed additives. If they are present, their concentrations should be so low that they should not increase concentrations of regulated materials in TCLP leachates above regulatory levels. Additionally, none of the additives contain organic compounds that are suspected to produce decomposition by-products regulated under the EPA's Toxicity Characteristic criteria.

Handling Properties

Since the objective of using these additives is to enhance the adhesive properties of the flyash, their use may affect dry transport systems. Since dry transport systems rely on free flowing particles, the problems are likely to increase with the degree of cohesion attained. Testing would be required to characterize actual effects.

Disposal Properties

A primary concern for the disposal of flyash is its ability to develop strength in a landfill. Although only low levels of strength development are required for landfill disposal, the proposed additives have some potential for hindering strength development. Precipitation of calcium compounds is key to strength development. At the proposed levels of addition, the additives may or may not retard or hinder strength development in landfilled flyashes. The effects on strength development will primarily depend on an additive's complexing ability and concentration. Testing would be required to characterize these effects.

Reuse Potential

Currently, flyash is reused in cement and concrete production. The potential effects on reuse are the same as those for disposal properties. Once again, testing would be required to characterize these effects.

VIII. Evaluation of the Insitec Instrument

Introduction

To provide real-time feedback on the effects of the additives on ESP performance, ADA acquired a laser particle size and velocity measurement system: the Particle Concentration, Size, and Velocity instrument, model E (PCSV-E). The equipment is manufactured and sold by Insitec Measurement Systems of San Ramon, California. The hardware consists of a U-shaped bridge unit that houses the optics for a laser transmitter and receiver, a signal processing unit, and an advanced personal computer that performs the computations and displays measurement results. Insitec has also packaged software with the instrument to control the optical alignment, data acquisition, and analysis functions from the keyboard of the PC.

In conjunction with the PCSV-E system, shipping cases for both the bridge unit and the electronics/computer system were purchased. These are designed to protect and cushion the hardware during transportation to test sites.

The PCSV system was acquired in order to make flyash particle size, concentration and velocity measurements in flue gas streams both in the field and in the ADA laboratory. An initial test was scheduled to assess the performance of the instrument in comparison to conventional particle size and concentration sampling techniques; specifically, a modified EPA Method 17 for total particulate loading determination, and particle impactors and cyclones for size fractionation. Testing was performed on the inlet and outlet of a pilot-scale electrostatic precipitator (ESP) operated by Consolidation Coal Co. at their Research and Development Laboratory's Combustion Research Facility.

The comparison testing was performed on inlet and outlet ductwork to the ESP modified to accommodate measurements with the PCSV-E. While the laser instrument was in operation, simultaneous measurements were made with a modified Method 17 sampling system, SRI cyclone sampler, and both Anderson and University of Washington cascade impactors. Since the laser-based PCSV measurements are non-intrusive, the laser access ports were installed upstream of the sample ports for the standard methods. The laser access ports consisted of four inch pipe flanges on opposite sides of the ductwork, each fitted with an optical quartz viewport for transmission of the laser beam across the interior of the duct. A focal point in the laser beam defined the sample volume of the PCSV instrument in the duct interior, at the approximate center of the duct.

Modified Method 17 samples and size fraction impactors and cyclones were run on the inlet and outlet of the ESP during data acquisition with the Insitec instrument. The extractive samples were taken over 10-minute to two-hour intervals, while the PCSV laser measurements each required about five minutes to complete. Data was reduced by the organizations that operated the respective equipment, and was compiled by ADA so that comparisons could be made among the several types of equipment used.

Test Procedures

Several days were required for setup and installation of the equipment at the Consolidation Coal Co. Research and Development Labs. The most extensive effort was required for the layout and fabrication of platforms to support the PCSV-E optics bridge at the inlet and outlet of the ESP. These were built by welding Unistrut structural steel tubing to the ESP frame, and then using threaded rod inserted into Unistrut fittings to suspend a plywood platform on which the PCSV-E optics bridge was positioned. The window flanges were installed in 4 inch couplings previously welded into the eight inch flow duct.

The PCSV-E system was also unpacked, assembled, checked out and calibrated in this set-up period. The system was found to have survived the transportation to the test site, and required only a minor adjustment to the calibration. This recalibration was accomplished on-site with the calibration reticle supplied as part of the instrument hardware.

Since this was the first field test of the PCSV-E system for ADA, arrangements were made to have a factory technical representative on site to provide guidance and support in the operation of the system. The representative was present for the first two days of testing, and proved to be most valuable in providing insight into the optimization of system parameters during data acquisition with the instrument.

During initial operation of the PCSV-E on the inlet to the ESP, problems arose over the strength of the laser signal passing through the two viewports that sealed the flue gas flow from the ambient environment. These were planned to be optical quality quartz windows, but the vendor was unable to ship the components in time for initial testing. Windows fabricated from commercial float glass were used instead, and the attenuation of the laser beam was significant. A thinner type of float glass was installed, which brought the laser beam intensity up to a minimal level required for normal operation of the PCSV system.

The optical quartz windows were delivered on the second day of testing, and were immediately installed. The measured laser beam intensity rose by about 50%, to operational levels that provided improved instrument resolution. Tests were conducted on both the inlet and outlet of the ESP with the quartz windows.

A second problem arose during Insitec measurements at the inlet to the ESP. Particle concentrations in the flow combined with the extended path length across which scattering could occur (recall that these measurements were made in an eight inch diameter duct) caused signal levels from scattered laser light to be so high that the system electronics were reaching saturation, and only a fraction of the particles were being counted. To address this problem, a modification was made to the quartz window installation flanges. A two inch diameter tube was welded to the window support flange to reduce the path length in which flyash particles attenuated the laser beam. The tubes extended about one inch into the flow path, and were purged with a low flow of dry nitrogen to reduce the particle count in the light path of the instrument. The external side of the fused quartz windows were maintained at elevated temperatures by directing a stream of air from a heat gun at each window. This eliminated the potential for condensation to form on the windows, which would attenuate the scattered light signal to below detectable levels.

In order to make measurements over a wide range of particle sizes, the Insitec instrument is built with two sets of laser optics. One set provides a larger diameter beam to obtain data on particles in the range of 5 to 150 microns, and the second forms a smaller diameter beam for measurement of particles from 0.4 to about 3 microns in diameter.

A full data run with the Insitec instrument requires the acquisition of four separate data samples. Because the velocity of particles in the flow is a term used in the calculation of particle size distribution, velocity measurements are made with both the large and small laser beams to comprise two of the four data samples. The remaining two samples (one taken with each size laser beam) acquire scattered light intensity data that is separated into bins that represent discrete levels of intensity of the scattered light. The deconvolution algorithm is then applied to the scattered intensity arrays to compute particle size and concentration distributions. Another algorithm is used to interpolate between the minimum size measured with the large beam and the maximum size of the small beam.

A total of 66 runs were made with the Insitec instrument, where measurements were made on both the inlet and outlet ducts of the CONSOL ESP. Of these, 25 runs were conducted on the outlet, and 41 runs on the inlet of the ESP. The inlet runs were divided into two groups, one where float glass windows were used (18 runs) and the scattered light signal was at minimum acceptable levels, and a second group of 23 runs where the optical quartz windows were installed, and the light levels increased by about 50% over the minimum level of the earlier measurements.

Data from the Insitec instrument is available immediately after completion of the data samples, while the standard techniques require significant effort to reduce the data to usable numbers. The Insitec information is saved to a computer file, which can be transferred to a spreadsheet for additional analysis and comparison to the physical sampling results.

The sampling crew from CONSOL obtained samples on all three days where Insitec data was taken. Their tests included 7 modified Method 17 total particulate samples, 3 cyclone size distribution samples and 3 Anderson impactor size distribution samples. The modified Method 17 data was reduced immediately, and is included in the data presented here. The EPA standard for Method 17 sampling specifies that the filter be inside the duct being sampled; this was not practical for the 8 inch diameter duct at CONSOL, so the filter was located in a heated housing external to the duct. The modified Method 17 probes were traversed across the duct at specified locations to obtain a representative sample in the flow.

ADA Technologies also performed extractive sampling, running a total of 7 University of Washington (UW) cascade impactors. Two of the impactor runs proved to be non-isokinetic, and were eliminated from the data set. Impactors are run at a single location in the flow because the size cuts of the various stages are functions of the flow through the device, which must remain constant throughout the run in order maintain constant size cuts among the stages.

Inlet Measurements

Summaries of the comparison of results from the modified Method 17 samples and the Insitec instrument are presented in Table VIII-1 for measurements made at the inlet to the CONSOL pilot-scale ESP. Data are shown for 3 Method 17 total particulate samples, along with corresponding Insitec runs.

Table VIII-1. Comparison of Modified Method 17 and Insitec Samples at the Inlet to the ESP

Sample ID	Measured Loading		Standard Loading (mg/dscm)	Measured Velocity (m/s)	Corrected Loading (mg/dscm)
	(gr/dscf)	(g/cc)			
Method 17 #2-Inlet	0.6886		1575.8	5.8	1575.8
Insitec C06 [Total]		7.71E-06	12197.7	4.9	10304.9
Insitec C07 [Total]		6.22E-06	9840.4	4.9	8313.4
Insitec C08 [Total]		6.98E-06	11042.8	5.0	9519.6
Insitec C09 [Total]		7.95E-06	12577.4	4.9	10625.7
Insitec C06 [<10 um]		6.01E-07	950.8	4.9	803.3
Insitec C07 [<10 um]		6.47E-07	1023.6	4.9	864.8
Insitec C08 [<10 um]		7.8E-07	1234.0	5.0	1063.8
Insitec C09 [<10 um]		4.63E-07	732.5	4.9	618.8
Insitec Avg. [<10 um]					837.7
Inlet #2 [<10 um]			1575.8		1008.5
Method 17 #3-Inlet	0.6837		1564.6	5.8	1564.6
Insitec C13 [Total]		9.25E-06	14546.2	5.0	12539.8
Insitec C14 [Total]		1.15E-05	18084.5	4.9	15278.3
Insitec C15 [Total]		9.51E-06	14955.1	5.0	12892.3
Insitec C13 [<10 um]		6.97E-07	1096.1	5.0	944.9
Insitec C14 [<10 um]		5.02E-07	789.4	4.9	666.9
Insitec C15 [<10 um]		7.88E-07	1239.2	5.0	1068.3
Insitec Avg. [<10 um]					893.4
Inlet #3 [<10 um]			1564.6		1001.3
Method 17 #7-Inlet	0.6172		1412.4	6.2	1412.4
Insitec C52 [Total]		4.41E-06	6895.8	4.7	5227.5
Insitec C53 [Total]		4.83E-06	7552.6	4.7	5725.3
Insitec C54 [Total]		4.74E-06	7411.8	4.9	5857.7
Insitec C55 [Total]		5.49E-06	8584.6	4.9	6784.6
Insitec C52 [<10 um]		5.13E-07	802.2	4.7	608.1
Insitec C53 [<10 um]		4.35E-07	680.2	4.7	515.6
Insitec C54 [<10 um]		4.12E-07	644.2	4.9	509.2
Insitec C55 [<10 um]		4.56E-07	713.0	4.9	563.5
Insitec Avg. [<10 um]					549.1
Inlet #7 [<10 um]			1412.4		903.9

The Insitec data are reported as grams of particulate matter per actual cubic centimeter of flue gas, and are therefore recalculated to match the milligrams per dry standard cubic meter in which the Method 17 data are reported. The calculation is performed by accounting for the sampling conditions at the time that the samples were taken. These were included in the data set for the Method 17 samples, so that it was possible to restate the Insitec values to standard gas conditions. It must also be noted that the "Measured Loading" column for the Insitec samples reports values that assume a particle density of 1 gram per cubic centimeter; this is not the correct density for the flyash at CONSOL, but was used so that a density correction could be determined from a flyash sample and easily applied to the data when the analysis was performed. A sample of ash was analyzed in the ADA laboratory using a helium pycnometer; the density of the flyash particles was found to be about 2.5 g/cc. This density and the corrections to standard conditions are applied to obtain the values in the column labeled "Standard Loading".

An additional correction was applied to the data from the Insitec instrument. The instrument measures the frequency distribution of particle sizes over a timed interval, and then computes the concentration by calculating the total volume of particulate matter, multiplying this volume by the particle density input to the software, and using the Insitec-measured velocity to determine the flue gas volume passing through the laser beam sample location in the timed interval. It was noted that the Insitec instrument consistently reported particle velocities in the duct that were about 20% below pitot measurements at the inlet and about 10% low at the outlet. To account for this difference, the Insitec data was corrected in the final column of the table through multiplication of the "standard loading" by a ratio of the Insitec velocity to the measured pitot velocity.

Each modified Method 17 sample is grouped with the Insitec runs taken during the time period over which the Method 17 sample was obtained. Recall that a typical Insitec run takes about 5 minutes, while the modified Method 17 samples ran about an hour.

At first glance, the Insitec instrument appears to measure much greater concentrations than the Method 17 samples at the inlet. This is due to a factor first reported by Holve, et al. [1988], where large flyash particles scatter laser light more efficiently than particles below 15 microns in diameter. The result is that the Insitec software calculates the sizes of these more-efficient scattering particles as larger than their actual dimension. The impact is further aggravated by the fact that many of these large particles are unburned carbon or spherical shells rather than high-density flyash material [Bonin and Queiroz, 1992]. The particle fractions greater than 15 microns in diameter thus are reported as oversized by the Insitec and also as comprising a majority of the total mass loading at the inlet.

In order to make a more meaningful comparison of the Insitec and modified Method 17 results, the size distribution information of the Insitec was employed. In an ESP, the most significant size region in terms of collection is the fraction below 10 microns in diameter. Those particles greater than 10 microns are almost certain to be collected because of their relatively large size and ease of charging; the particles that resist collection are invariably those below 10 microns. This is confirmed in the Insitec measurements made on the outlet from the ESP. The largest particles reported by the Insitec for the runs that corresponded to the modified Method 17 samples at the outlet were between about 7 and 13 microns in diameter; this is in great contrast to the inlet where particles greater than 100 microns in size were routinely reported in the Insitec data sets.

For the inlet to the CONSOL ESP, there were multiple Insitec runs for each modified Method 17 sample. Table VIII-1 lists the corresponding Insitec results for each Method 17 sample, and also presents the fraction of particulate matter below 10 microns in diameter for the Insitec runs. The data files for the Insitec runs present a tabulated distribution of mass loading as a function of particle size. Information for the table was taken directly from the Insitec tabulated data. A 10-micron cut value for the modified Method 17 samples was calculated by visually fitting a line to impactor data for the inlet, plotted on a log-probability graph. The mass fraction less than 10 microns was then defined as the value where the fit-line crossed the 10 micron line on the graph. This fraction was found to be 0.64 for the inlet UW impactor runs; the total standard loading for the modified Method 17 sample was then multiplied by 0.64 to obtain a mass fraction less than 10 microns.

The mass fraction less than 10 microns in diameter are seen to compare quite well. In almost all cases, the Insitec values are less than the modified Method 17 numbers. The averages of the Insitec data are within 20% of the modified Method 17 measurements for the first two samples, and within 40% for the final sample. The modified Method 17 samples showed about a 10% difference between the largest and smallest measured loading, so that there is some natural variation present in the flow stream. This variation is emphasized in the Insitec samples because of their relatively short time duration. The hour-long sample time of the modified Method 17 samples tends to average more transient oscillations in the flyash concentration; the Insitec runs take about 5 minutes, where 2 minutes is actual data acquisition time for the particle sizing data.

A comparison of measured size distributions for the University of Washington impactor, the Anderson impactor and a typical Insitec run is shown in Figure VIII-1. The two impactors are seen to be quite similar in their measured distributions. The Insitec has a minimum detectable size of about 1.6 microns, because of the laser attenuation at the inlet due to particle concentration and optical path length. For the size range over which comparisons can be made, the Insitec has a shape similar to the impactor data. When the offset due to minimum detection size of the Insitec is considered, the profile is seen to be very similar to the impactor results.

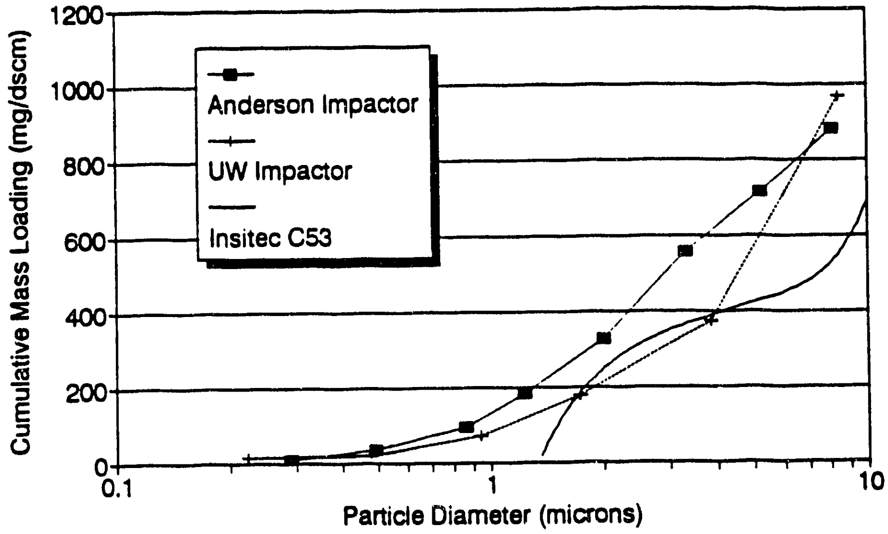

Figure VIII-1. Comparison of Measured Size Distributions for the ESP Inlet.

Outlet Measurements

Table VIII-2 presents the comparison of data for the modified Method 17 samples taken at the ESP outlet and Insitec runs made through measurement ports upstream of the outlet sample point. The format is identical to the earlier inlet data, with the Insitec data restated to standard conditions and corrected for a difference in measured velocity between the Insitec and a pitot probe at the modified Method 17 location. There is a value presented for the modified Method 17 fraction below 10 microns that is derived from a visual linear fit to the ADA University of Washington impactor results, plotted as a log-probability function. This fit predicted that 89% of the total captured mass was of a diameter below 10 microns. The total modified Method 17 mass loading was thus multiplied by 0.89 to compute the fraction below 10 microns.

Table VIII-2 Comparison of Modified Method 17 and Insitec Samples at the Outlet to the ESP

	Measured Loading		Standard Loading	Measured Velocity	Corrected Loading
Sample ID	(gr/dscf)	(g/cc)	(mg/dscm	(m/s)	(mg/dscm)
Method 17 #4-Outlet	0.0243		55.6	5.9	55.6
Insitec C20 [Total]		2.38E-08	38.5	5.6	36.6
Insitec C20 [<10 um]		2.38E-08	38.5	5.6	36.6
Outlet #4 [<10 um]			55.6		49.5
Method 17 #5-Outlet	0.0090		20.6	6.0	20.6
Insitec C27 [Total]		1.6E-08	26.1	5.4	23.5
Insitec C28 [Total]		8.32E-09	13.6	5.4	12.2
Insitec C29 [Total]		1.22E-08	19.9	5.3	17.6
Insitec C30 [Total]		1.9E-08	31.0	5.4	27.9
Insitec C27 [<10 um]		1.58E-08	25.8	5.4	23.2
Insitec C28 [<10 um]		8.32E-09	13.6	5.4	12.2
Insitec C29 [<10 um]		1.22E-08	19.9	5.3	17.6
Insitec C30 [<10 um]		1.87E-08	30.5	5.4	27.5
Insitec Avg. [<10 um]					20.1
Outlet #5 [<10 um]			20.6		18.3
Method 5 #6 Outlet	0.0126		28.8	6.6	28.8
Insitec C31 [Total]		2.83E-08	45.1	5.3	36.3
Insitec C32 [Total]		1.26E-08	20.1	5.4	16.4
Insitec C33 [Total]		1.8E-08	28.7	5.3	23.1
Insitec C34 [Total]		2.08E-08	33.2	5.3	26.6
Insitec C31 [<10 um]		2.8E-08	44.7	5.3	35.9
Insitec C32 [<10 um]		1.26E-08	20.1	5.4	16.4
Insitec C33 [<10 um]		1.8E-08	28.7	5.3	23.1
Insitec C34 [<10 um]		2.05E-08	32.7	5.3	26.3
Insitec Avg. [<10 um]					25.4
Outlet #6 [<10 um]			28.8		25.7

The Insitec data for the outlet agrees quite well with the modified Method 17 results. Averages were calculated for multiple Insitec runs obtained during the 60 minute Method 17 sample period. These are included in the table, and are seen to be within 30% in the worst case, and within 1.5% for the best case. There is also an obvious significant variance in the outlet loading; this may be a function of rapping time with respect to sampling time for the modified Method 17 tests. There also appears to be better agreement at lower loading values. This is significant in the use of the Insitec to quantify performance of additives to enhance ESP performance, since a successful additive will reduce the outlet loading from the ESP in comparison the loading at normal operating conditions.

In Figure VIII-2, results of two different impactor runs are compared with a corresponding Insitec size distribution over the diameter range of interest of 0.1 to 10 microns. The distributions compare favorably, although the Insitec measures higher loading in the region around 1 micron. It must be noted, however, that the impactor distribution is plotted for 50% cut points, so that there is some broadening in the size bands of the impactor data. The lower limit of detection for the Insitec is about 0.4 microns, so there is no data available for comparison to the final two stages of the UW impactor. The offset for the outlet is less significant than at the inlet because of the lower minimum diameter detected by the Insitec instrument.

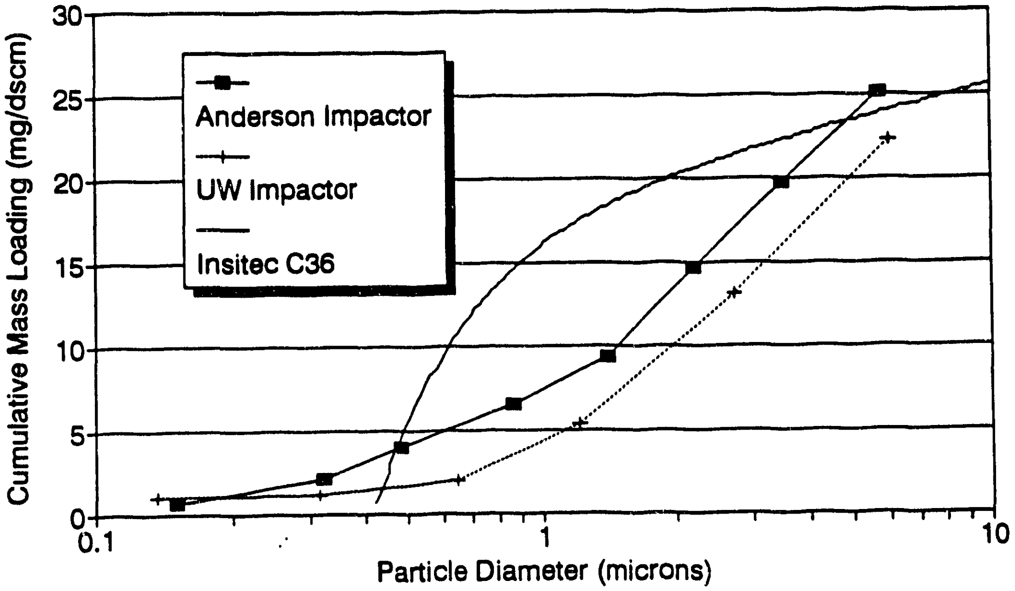

Figure VIII-2. Comparison of Measured Size Distributions for the ESP Outlet.

Conclusions and Recommendations

The Insitec Particle Concentration, Size, and Velocity instrument was used to measure flyash particle size distributions and concentrations at the inlet and outlet of an operating ESP. The results were compared with extractive samples taken following a modified EPA Method 17 protocol for particle loading measurements and cyclones and cascade impactors for size distribution data. The Insitec results at the inlet to the ESP present high values for mass loading, due to the detection of large numbers of large particles. This information is subject to interpretation at two levels: first, the larger particles in the flue gas stream tend to be unburned carbon or shell-type spherical particles which scatter the laser illumination of the Insitec instrument more like a transparent particle than an opaque particle that is assumed in the analysis routine. Second, these shell-type particles are most certainly not the density of the smaller particles, which form most of the mass and are used in the determination of density for the flyash. These large particles are thus not as large nor as dense as assumed in the Insitec computer analysis.

The results of these measurements are summarized in Table VIII-3. The Insitec data was shown to be very consistent from run to run, and to compare favorably with the particle loading measurements at sizes less than 10 microns. This is the size range of interest, because larger particles are assured of capture in a properly operating ESP. Based upon these results it appears that the Insitec instrument would be very useful for providing real time data on both mass and particle size distribution for particles less than 10 microns.

References

Holve, D.J., P.L. Meyer, L.J. Muzio, and G.H. Shiomoto, (1988). "On-Line, In-Situ Particle Measurements in a Large Scale Coal-Fired Furnace". Paper #88-60, Western States Section of the Combustion Institute, Salt Lake City, UT, March.

Bonin, M.P. and M. Queiroz (1992). "A Parametric Evaluation of Particle Phase Dynamics in an Industrial-Scale, Coal-Fired Boiler". Submitted for publication.

Table VIII-3. Summary of the Comparisons between Method 17 and Insitec for Particles Less than 10 Micrometers in Diameter.

	Method 17 (mg/dscm)	Insitec (mg/dscm)
Inlet	1008.5	832.7
Inlet	1001.3	893.4
Inlet	903.9	549.1
Outlet	49.5	36.6
Outlet	18.3	20.1
Outlet	25.7	25.4

IX. Economic Analysis

Mr. Victor Belba will be performing an initial economic analysis with the purpose of determining whether any of the additives identified for bench-scale testing should be eliminated from further consideration due to potential excessive costs. The costs associated with the additives will be compared against cost of adding ESP capacity to produce a comparable improvement in particle collection capability. The initial analysis will be performed using data generated from the laboratory testing and will be scaled for a plant of 250 MW in size. Elements of the analysis will include the following items:

- Obtaining preliminary capital and operating costs for an injection system.
- Obtaining information on the additives relative to form (bulk solid or concentrated liquid), special handling procedures, storage constraints, and costs.
- Determining projected consumption rates for the different additives and estimating particle capture improvements.
- Determining the additional specific collection area increase needed in an ESP to produce a comparable improvement in particle collection.

X. Conclusions and Recommendations

Following are conclusions and recommendations resulting from the program to date:

- A total of 31 additives were investigated in screening and laboratory-scale precipitation tests.
- Four additives have been identified and are recommended for further testing at bench-scale.
- The laboratory-scale test apparatus has been perfected and gives consistent and reproducible test conditions.
- Initial analysis of projected waste characteristics indicates that the additives will not impact the options for waste disposal, ash handling, or ash reuse.
- The Insitec analyzer will be an acceptable tool for the program in evaluating additive performance for particles less than 10 μm in diameter.

END

DATE
FILMED

7/12/93